Imperial College London
Department of Physics
Theoretical Physics Group

What We Have Learned of Quantum Gravity From Holography

Author: Abdulaziz Bazammul
Supervisor: Prof. Toby Wiseman

Submitted in part fulfilment of the requirements for the degree of
Master of Science of Imperial College London

Abstract

The existence of a correspondence between quantum and gravitational theories has been conjectured for a long time. The conjecture began with Super Yang Mills gauge theories as the quantum theories, and D-P branes string theories as the gravitational theories. Since then, the conjecture has developed greatly. The aim of this dissertation is to explore this development. To do this, we first start by setting some background information regarding the holographinc principal and quantum gravitational theories followed by a brief black holes thermodynamics review. We then start by explaining the gauge/gravity duality followed by a journey through the various models ranging from the very first proposed model of the conjecture (BFSS) and going through much later developed models like BMN. We then see the conjecture being evolved to the point where the quantum theories are ungauged. Ending with the simplest model to date, in which the quantum theory is a simple quantum mechanical system and the gravitational theory is a black hole. We then see the important role to be played by quantum simulation in order to advance this field of literature further.

Acknowledgements

I would like to express my deepest gratitude to Prof. Toby Wiseman for his unwavering support and invaluable guidance throughout the journey of writing this dissertation. Prof. Wiseman's expertise, dedication, and responsiveness have been instrumental in shaping this work. His insightful feedback, constructive criticism, and encouragement have enriched the quality of my writing. I am truly fortunate to have had the privilege of working under Prof. Wiseman's supervision, and his mentorship has been a source of inspiration. I extend my heartfelt thanks for his commitment to my academic growth and for making this dissertation possible.

I would also like to express my heartfelt gratitude to King Abdulaziz University, particularly the Physics Department, for their unwavering support throughout my scholarship period. Your generosity has not only relieved the financial burden of higher education but has also provided me with an exceptional academic environment. The guidance, resources, and mentorship from the faculty and staff have been invaluable in my academic growth, and the collaborative spirit among my peers has made my journey enjoyable. I am committed to using the knowledge and skills gained here to make a positive impact on society. Thank you for this life-changing opportunity.

A special thanks is on order for my friends, Mohammed and Jack. Their impact on my performance during this masters can not be denied. I will forever be grateful to them.

Dedication

To My Dearest Family, Friends, and Loved Ones,

As I embark on this journey, I want to take a moment to express my deepest gratitude and love for each of you. This endeavor, which represents a significant chapter in my life, would not have been possible without your unwavering support, encouragement, and belief in me.

To my family, you have never stopped supporting me. Even while I was away and far from home, your continuous care and support have had a tremendous positive impact on my mental strength. This achievement is as much yours as it is mine.

To my friends, you have been my companions through thick and thin. Your laughter, shared experiences, and the countless late-night discussions have added depth to my life. Your friendship has been a source of inspiration and resilience.

To my loved ones, you have filled my life with warmth, affection, and countless cherished moments. Your unwavering belief in me has been a source of motivation. Your presence has illuminated my path and made this journey more meaningful.

This dissertation is not just a culmination of my efforts; it is a reflection of the collective support and love that you have showered upon me. It stands as a testament to the strength of our bonds and the power of shared dreams.

Thank you for being my pillars of strength, my companions in joy, and my solace in times of need. This achievement is a tribute to our unity, and I look forward to sharing the joys of this accomplishment with you.

With all my love and gratitude,

Abdulaziz.

Contents

Chapter 1

Introduction

On the holographic principal and quantum gravity

The pursuit of understanding the fundamental nature of the universe has been an unending journey for scientists and physicists throughout history. At the heart of modern physics, two dominant theories, quantum mechanics and general relativity, stand as monumental achievements, yet they pose a daunting challenge at their interface, where quantum mechanics and gravity intersect. In this challenging terrain, the Holographic Principle emerges as a guiding light, offering a path toward reconciling these seemingly disparate realms. This introduction embarks on a comprehensive exploration of the Holographic Principle, its revolutionary implications, and its deep-seated relationship with the elusive domain of quantum gravity. We will also delve into the groundbreaking contributions of Juan Maldacena and his transformative impact on the field.

At its core, the Holographic Principle challenges the foundational principles of our understanding of reality. It posits that all the information contained within a three-dimensional volume can be entirely encoded on a two-dimensional surface that surrounds it. In simpler terms, it suggests that the complete physical description of a given space can be equivalently expressed on its boundary, much like a hologram reconstructs a three-dimensional image from a

two-dimensional surface.

The roots of the Holographic Principle extend back to the late 20th century when theoretical physicists Tom Banks, Willy Fischler, Stephen Shenker, and Leonard Susskind began to explore this revolutionary concept[3, 75]. However, its most significant advancement came with the groundbreaking work of Juan Maldacena in 1997 [47].

Juan Maldacena's contribution to the Holographic Principle, incarnated by the AdS/CFT (Anti-de Sitter/Conformal Field Theory) correspondence, represents a milestone moment in theoretical physics. The AdS/CFT correspondence unveiled a profound duality between a higher-dimensional gravitational theory, particularly string theory or M-theory in an anti-de Sitter space (AdS), and a lower-dimensional conformal field theory (CFT) residing on the boundary of that AdS space. This groundbreaking revelation dramatically shifted our perspective on the relationship between quantum mechanics and gravity. The AdS/CFT correspondence essentially posits that the complex and intricate world of quantum gravity in higher-dimensional spaces can be precisely captured and understood through a simpler, lower-dimensional quantum field theory. This correspondence has opened up an entirely new and potent tool for investigating the profound nature of quantum gravity without diving deeper into the complexities of higher-dimensional spacetimes.

As we venture deeper into the holographic frontier, we continue to uncover remarkable insights into the interconnectedness of fundamental physics. The Holographic Principle has become a guiding star in our pursuit of a comprehensive theory that unifies the quantum world and gravity. This journey has implications not only for theoretical physics but also for our understanding of the universe itself. The Holographic Principle challenges our perceptions of reality and suggests that the true nature of the cosmos may be more intricate and interconnected than we had ever imagined.

As mentioned earlier, the achievements of the Holographic Principal along with the works of Juan Maldacena enabled us to explore complex high-dimensional theories through the eyes of a, much simpler, lower-dimensional one. It is this simplicity that will be the main focus here, this dissertation will explore various models that have their origins in string theory but can be understood through a quantum mechanical regime. We will avoid string theory discussions where possible and try to shed more light to the quantum mechanical formulation and its duality to a gravitational one.

Our heated discussion of these models begins in chapter 3. Before that, we would like to cover some important black hole concepts that plays a central role in understanding this piece of literature. Namely, we would like to talk about black hole thermodynamics and the information paradox. This will be done in chapter 2. In chapter 4, we will discuss what to expect next following the models of chapter 3.

Chapter 2

On Black Holes

Before delving into the intricacies of black hole entropy, it is essential to grasp the concept of entropy itself. In physics, entropy is a measure of the disorder or randomness of a system. It is often associated with the second law of thermodynamics, which states that the total entropy of an isolated system will tend to increase over time, ultimately leading to a state of maximum entropy, known as thermodynamic equilibrium.

In classical thermodynamics, entropy is usually associated with the behavior of gases, heat transfer, and energy dissipation. However, the notion of entropy extends far beyond classical thermodynamics and plays a significant role in various branches of physics, including quantum gravity.

The concept of black hole entropy emerged as a paradoxical and groundbreaking discovery in the mid-20th century. The story begins with the work of Jacob Bekenstein in the early 1970s [5]. Bekenstein postulated that black holes must have an associated entropy, challenging the common belief that black holes were entirely unlinked to any thermodynamic properties. He proposed that the entropy of a black hole was proportional to its surface area, measured in Planck units, a fundamental scale of nature derived from quantum mechanics.

The concept of black hole entropy gained further support and prominence with Stephen Hawking's groundbreaking work on black hole evaporation in 1975 [36]. Hawking's calculations

demonstrated that black holes were not entirely black[1]; instead, they emitted a faint but steady stream of particles, now known as Hawking radiation. This emission process gradually led to the reduction of a black hole's mass and, eventually, its complete evaporation.

Hawking's discovery was a triumphant moment in physics, as it marked the first successful attempt to reconcile quantum mechanics with the profound gravitational effects near a black hole's event horizon. Hawking radiation introduced quantum effects into the realm of gravity, highlighting the need for a theory that could unify these two disparate worlds, a theory now known as quantum gravity.

The interplay between black hole entropy and quantum mechanics gave rise to one of the most enduring puzzles in modern physics, the black hole information paradox. This paradox posits that the information that falls into a black hole, such as the quantum state of matter and radiation, appears to be lost forever once the black hole has completely evaporated. This apparent violation of the fundamental principles of quantum mechanics, which dictate that information cannot be destroyed, led to intense discussions and debate within the physics community.

The resolution of the black hole information paradox is intimately tied to the quest for a theory of quantum gravity. Physicists have explored various avenues to address this paradox, including string theory, loop quantum gravity, and holography, the latter of which we discussed earlier in relation to the Holographic Principle. These theories seek to reconcile the quantum behavior of matter and fields with the gravitational effects near black holes, ultimately preserving the unitarity of quantum mechanics.

Black hole entropy, with its profound implications and connections to quantum gravity, serves as a powerful reminder of the profound mysteries that persist at the intersection of these two fundamental theories. The exploration of black hole entropy has reshaped our understanding of black holes, thermodynamics, and the fundamental nature of the universe itself.

While significant progress has been made in unraveling the mysteries surrounding black hole

[1] By "entirely black" we mean a body that absorbs everything and emits nothing

entropy, the full resolution of the black hole information paradox and the attainment of a comprehensive theory of quantum gravity remain elusive goals. The quest for a unified theory that harmonizes the quantum and gravitational worlds continues to drive the work of physicists, offering the promise of deeper insights into the fundamental laws that govern our universe.

With this being said, our main aim in this chapter is to unravel the aforementioned black hole properties. Setting a common ground for our later discussions about holographic models in chapter 3.

2.1 Thermodynamics and entropy

We begin with a brief derivation of Hawking's temperature using quantum mechanical principals [56]. The uncertainty principal states

$$\Delta x \Delta \nu = \frac{\hbar}{2m} \tag{2.1}$$

where Δx is the uncertainty in the position of the particle and $\Delta \nu$ is the uncertainty in its speed. Equation (2.1) gives the minimum value that the product of these quantities can take. Recalling the relativistic relation between the mass m and energy E of a particle: $E = mc^2$. Hence,

$$\Delta x \Delta \nu = \frac{c^2 \hbar}{2E} \tag{2.2}$$

The previous two equations show that Δx and $\Delta \nu$ are inversely proportional. Because quantum black holes are very small, if a particle is inside one, the uncertainty in its position, Δx, becomes quite small. This means we can increase the uncertainty in its speed, $\Delta \nu$ to a level where it's greater than the speed of light c. When this happens, the particle can escape from the black hole and cross its boundary, known as the event horizon, to the outside.

Since quantum events are inherently uncertain or random, we can't predict with certainty which type of particle will escape or exactly when it will happen. However, over time, this randomness results in a continuous release of particles. These particles are emitted in various directions

away from the event horizon, and we refer to this phenomenon as Hawking radiation. As each particle escapes through Hawking radiation, it takes away a portion of the black hole's mass-energy, causing the black hole's mass, M_{BH}, to decrease gradually. This reduction initiates the process of black hole evaporation.

Since the emission of this radiation happens within the range of uncertainty related to speed, it's crucial to note that we cannot actually witness a particle moving faster than the speed of light. Therefore, from a practical standpoint, this mechanism doesn't lead to a violation of the principles of relativistic physics.

Let's delve into the details more precisely. Imagine a particle inside a stationary black hole. We know that how uncertain the particle's position, Δx, is depends on the black hole's size. Since we have some flexibility in determining this uncertainty, we can assume that Δx is equivalent to the circumference of the black hole's boundary, often referred to as the event horizon. We will use Shwarzchild's radius, $R_s = \frac{2GM_{BH}}{c^2}$ for convenience. Hence,

$$\Delta x \approx 2\pi R_s = \frac{4\pi G M_{BH}}{c^2} \tag{2.3}$$

where G is Newton's gravitational constant, M_{BH} is the black hole's mass and c is the speed of light. The crucial requirement for the particle to break free from the black hole is when $\Delta\nu$ equals the speed of light c. Applying this condition to Equation (2.2) and incorporating the outcome into Equation (2.3) yields

$$E = \frac{c^3\hbar}{8\pi G M_{BH}} \tag{2.4}$$

furthermore, we can impose a condition on energy since Hawking's radiation follows a thermal behaviour. Namely,

$$E \approx kT \tag{2.5}$$

where k is boltzman's constant and T is the absolute temperature. Hence, equation (2.4) results to

$$T = T_H = \frac{c^3\hbar}{8\pi k G M_{BH}} \tag{2.6}$$

It is worth noting that we will use natural units from now on unless stated otherwise. Writing

equation (2.6) in natural units

$$T_H = \frac{1}{8\pi G M_{BH}}. \tag{2.7}$$

Hence, we showed that Hawking's temperature could be derived using quantum mechanics.

Now, would like to discuss black hole entropy [33]. Since a black hole has temperature and energy, it is logical that it has entropy. Remember, in statistical mechanics, temperature is typically defined in relation to the entropy, S, as:

$$\frac{dS}{dE} = \frac{1}{T} \tag{2.8}$$

we have: $T = T_H = \frac{1}{8\pi G M_{BH}}$, $E = M_{BH}$ in natural units and assuming $S(E = 0) = 0$, yields

$$S = \frac{\text{Area}}{4G} = 2\pi \frac{A}{l_p^2} \tag{2.9}$$

where the area of the horizon is $4\pi R_s^2$ and $l_p = \sqrt{8\pi G}$ is the Planck length. This entropy is staggering in magnitude. For instance, for a black hole with the mass of our sun, it reaches around 10^{78}, significantly surpassing the entropy of the sun itself, which is approximately 10^{60}. To put it in perspective, the entropy of the entire observable universe, excluding black holes and mainly governed by cosmic microwave background photons, is roughly 10^{87}.

Comparatively, a single black hole with a mass equivalent to a million suns, like the one at the center of our Milky Way galaxy, possesses an entropy of roughly 10^{88}. When we consider the most massive supermassive black holes, which can have masses on the order of 10^{10} solar masses, their entropies reach levels around 10^{96}.

Regarding temperature, within classical general relativity, one can establish, under fairly broad assumptions, that the area of an event horizon never diminishes over time [35]. This property bears a resemblance to the second law of thermodynamics. If we formally introduce an entropy proportional to the horizon area and a temperature on the order of 1 divided by the Schwarzschild radius ($1/R_S$), we find that a first law of thermodynamics, expressed as

$dM_{BH} = TdS$, is also satisfied [5, 4].

Bardeen, Carter, and Hawking initially regarded this as a mere mathematical analogy [4]. However, Jacob Bekenstein of the Hebrew University took a different stance, suggesting that this entropy should genuinely represent the statistical entropy of a black hole. He envisioned this as a way of counting the various possible manners in which a black hole could form [6]. Bekenstein argued that the entropy should be a constant multiple of the horizon area in Planck units and provided supporting evidence by examining hypothetical scenarios involving an entropic system being absorbed by a black hole. In each case, he observed that the black hole's entropy, defined in this manner, always increased more than the exterior entropy decreased due to the loss of the system. Bekenstein termed this observation the Generalized Second Law and conjectured that it held as a general principle [38, 6]. It was at this point that Hawking's paper on temperature completed the circle. Consequently, the quantity (2.9) is commonly referred to as the Bekenstein-Hawking entropy.

The proposition that the Bekenstein-Hawking entropy serves as a microstate enumerator has gathered robust backing within the framework of string theory. This theoretical framework, renowned for its profound contributions to the understanding of quantum gravity over the past few decades [57, 58], establishes arguments grounded in the enumeration of states inherent to a longitudinally oscillating string. These arguments have exhibited the capacity to deduce the area-dependent scaling pattern, as encapsulated in equation (2.9), across a comprehensive array of scenarios [73, 38]. Furthermore, within specific instances characterized by supersymmetry [72], these arguments achieved the precision required to compute the numerical coefficient similar to the 1/4 factor found in equation (2.9).

2.2 The information problem and black hole evaporation

We have now observed that black holes exhibit many thermodynamic characteristics. Following Bekenstein's pioneering work, it becomes almost irresistible to adopt the perspective that the Bekenstein-Hawking formula genuinely quantifies the logarithm of the count of microstates

corresponding to a black hole of a specific size.

However, let's momentarily consider an alternative viewpoint—one that insists black holes are primarily characterized solely by their mass (and potentially their charge and angular momentum, if these are taken into account), as suggested by the principles of general relativity. This perspective leads to a fundamental conflict with a basic principle in physics: the idea that if we possess knowledge about a system's state at a particular moment, we should be capable of deducing its initial state by running the system's dynamics backward in time.

This proposal essentially implies that by creating a black hole, we obliterate most of the information concerning the process that formed it. Since we are inclined to uphold this fundamental principle, we are naturally compelled to assume that black holes indeed possess microstates.

However, in a profoundly remarkable paper authored by Hawking [36], it is brilliantly argued that even when we allow for the possibility of black hole evaporation, this assumption alone is insufficient to prevent the loss or destruction of information.

Before delving into Hawking's argument, it's worth taking a moment to discuss the concept of information preservation. In classical mechanics, the progression of time is determined by Hamiltonian dynamics in phase space, which can always be reverted by simply changing the Hamiltonian's sign. More straightforwardly, we can solve the equations of motion backward in time. Similarly, in the realm of quantum mechanics, time evolution is described as unitary evolution within Hilbert space, and this too can be reversed by changing the sign of the Hamiltonian. It's important to note that these principles hold true only when the system in question is isolated; otherwise, information can escape or be lost.

The quantum case may appear somewhat counter-intuitive, primarily because the process of measurement is non-deterministic. However, it's crucial to recognize that every measurement entails the coupling of the system being measured with an external apparatus. Consequently, the evolution of this combined system remains both unitary and deterministic.

Now consider a black hole that was formed by a shell of matter in some pure quantum state $|\psi\rangle$. As time progresses, the quantum state of the radiation field surrounding the black hole

gradually becomes increasingly entangled or mixed. This can be quantified by noting that its entanglement entropy is on the rise. Initially, this might not appear concerning, as we are, after all, examining the radiation that exists outside the black hole's event horizon.

However, as the black hole undergoes evaporation, its size diminishes, eventually reaching a point where it becomes extremely tiny, on the scale of the Planck length. At this point one of two things must happen:

- The process of evaporation comes to a halt, and the exceedingly small Planck-sized entity remains in a steady state. This scenario is referred to as a *remnant*. For the entire system's quantum state to remain in a pure state, as mandated for unitary evolution, the remnant must possess an exceptionally high level of entanglement entropy. Even before it reaches the Planck size, the entanglement entropy of the remnant would need to surpass the Bekenstein-Hawking value. Such a situation would contradict the interpretation of (2.9) related to counting the states.

- The black hole completes its evaporation, transforming into particles like photons and gravitons. Due to energy conservation, the ultimate emission of these particles lacks the necessary entanglement entropy to cleanse the earlier radiation fully. Consequently, the outcome of the evaporation process is a radiation field in a mixed state, characterized by an entropy magnitude approximately equivalent to the initial black hole's event horizon area in Planck units.

Hawking put forward the second possibility. He argued that the way black holes form and eventually disappear doesn't follow a clear and consistent pattern where all the information is preserved. If it did, the radiation coming out would be in a pure state. But because different starting conditions can lead to the same result, Hawking suggested that black holes break the rule of keeping all information intact. So, this second option is often called *information loss*.

Fundamental laws of physics are typically not discarded unless it becomes evident that there are no other viable alternatives. How can we potentially sidestep the problem of information loss? While the first option is theoretically feasible, it's deemed unattractive because it necessitates

objects with finite energy but an infinite array of states. Consequently, it has rarely been seriously considered [61, 26, 74].

For those unwilling to embrace the idea of information loss, an alternative option, a third one, has gathered more attention.

- Equation (2.9) should be understood primarily as an approximation. In reality, Hawking radiation doesn't emerge in a truly mixed state. The information is conveyed through intricate correlations among the Hawking photons, and the ultimate state of the evaporation represents a pure state of the radiation field. Given its complexity, when we examine small portions of this system, they appear thermal, which justifies the reasonably accurate application of (2.9) as long as we're not considering too many photons simultaneously. There is a complete basis of such pure states whose dimensionality is the exponential of the Bekenstein-Hawking formula, which thus can indeed be interpreted as counting microstates. In this sense, equation (2.9) is called the *coarse-grained* entropy.

Option (3) might initially appear to be the most favorable choice among the three, but it entails a more profound departure from conventional thinking than it might seem at first glance. Equation (2.9) appears to be a consequence of widely accepted principles regarding the applicability of quantum field theory on scales significantly larger than the Planck scale. If this equation were incorrect, shouldn't we expect to detect this deviation from quantum field theory in other aspects or observations? Since each of the three options has its own unattractive characteristics, this situation is denoted as *the black hole information problem.*

Chapter 3

Models of Holographic Quantum Gravity

3.1 Gauge/Gravity duality explained

In this section, we delve into the concept of the gauge/gravity duality [48], which serves as a primary motivation for the exploration of black hole solutions in various dimensional contexts. The gauge/gravity duality represents an intriguing correspondence between two distinct theories: Firstly, we have a quantum field theory existing within d-dimensional spacetime. On the other side, we encounter a gravity theory inhabiting a $d+1$-dimensional spacetime, characterized by an asymptotic boundary of d dimensions. This duality is also frequently referred to as AdS/CFT, owing to its frequent association with anti-de-Sitter spaces and conformal field theories. Furthermore, it is often termed gauge-string duality, as it bridges the realm of quantum field theories, often involving gauge theories, with string theories embedded in gravity. An alternative name for this concept is "holography", drawing a parallel with optical holograms that encode three-dimensional images onto two-dimensional surfaces. Although initially proposed as a conjecture, substantial empirical evidence has since mounted in support of its validity, and it has been derived from physical arguments in various contexts. To commence our exploration, we will begin by providing a detailed exposition of anti-de-Sitter spacetime, which

serves as the foundational framework for many aspects of AdS/CFT. Anti-de-Sitter space is the most straightforward solution to Einstein's equations with a negative cosmological constant and can be thought of as the Lorentzian counterpart to hyperbolic space, which historically marked the inception of non-Euclidean geometries. Analogously, AdS/CFT furnishes us with a fundamental paradigm for understanding quantum aspects of spacetime.

3.1.1 Anti-de-Sitter spacetime

The metric in AdS space can be written as

$$ds^2_{\mathrm{AdS_{d+1}}} = L^2\bigg[-(r^2+1)dt^2 + \frac{dr^2}{r^2+1} + r^2 d\Omega^2_{d-1}\bigg] \tag{3.1}$$

where the last term is the metric of a unit sphere, S^{d-1}. L is the radius of curvature. Notice that in the vicinity of $r = 0$, the spacetime appears nearly flat. As we extend our scope to larger r values, it becomes evident that both g_{00} and the metric on the sphere experience an expansion. This expansion of g_{00} can be interpreted as an increase in the gravitational potential. To be precise, a slowly moving massive particle encounters a gravitational potential $V \sim \sqrt{-g_{00}}$. When a particle initially at rest is placed at a substantial r value, it initiates an oscillatory motion along the r direction, analogous to the behavior of a particle subjected to a harmonic oscillator potential. This gravitational potential effectively confines particles within the vicinity of the origin. In the case of a massive particle with finite energy, escape to infinity, $r = \infty$, becomes an impossibility. However, a massless geodesic has the capability to reach infinity and return within a finite period. An alternative perspective involves examining the Penrose diagram of AdS. By factoring out a term of $1 + r^2$ in the metric (3.1) and introducing a new radial coordinate, x, through $dx = dr/(1+r^2)$, which now exhibits a finite range. Consequently, the Penrose diagram of AdS space takes the form of a solid cylinder, as depicted in figure 3.1. In this diagram, the vertical direction corresponds to time, the boundary aligns with $r = \infty$, a finite value of x. The spatial section of the cylinder's surface represents S^{d-1}. While the metric in (3.1) notably possesses an evident $R \times SO(d)$ symmetry, AdS boasts a more extensive set of symmetries, specifically the full symmetry group $SO(2, d)$. These symmetries can be more

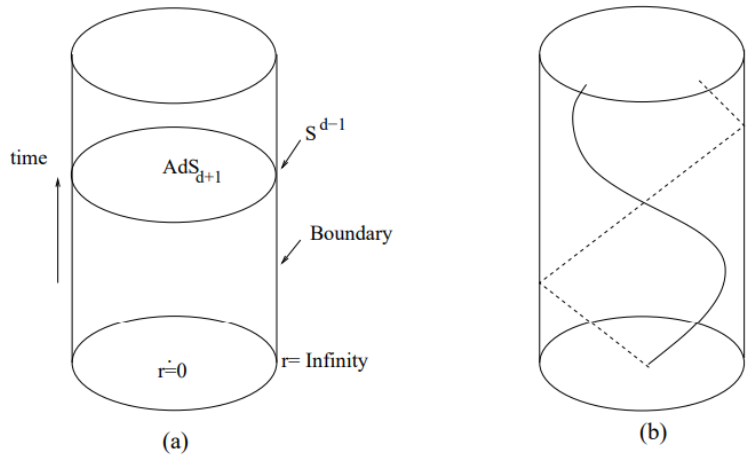

Figure 3.1: (a) Illustrated is the Penrose diagram for Anti-de-Sitter space, taking the form of a solid cylinder. In this diagram, the vertical axis corresponds to the temporal dimension. The boundary encompasses the temporal direction and includes a sphere, denoted as S^{d-1}, which is here represented as a circle. (b) The diagram portrays a massive geodesic trajectory using a solid line and a massless geodesic path using a dashed line for comparison. (Image credits: [48])

obvious by regarding AdS as the hyperboloid

$$-Y_{-1}^2 - Y_0^2 + Y_1^2 + \ldots Y_d^2 = -L^2 \tag{3.2}$$

in $R^{2,d}$. This depiction serves the purpose of explicitly grasping the symmetries. Nonetheless, within this hyperboloid, the temporal dimension, t, is compact (representing the angle within the [-1, 0] plane). However, in all physical contexts, we intend to consider this temporal direction as non-compact.

The isometries of Anti-de-Sitter space are of great importance. Let's recall the scenario in flat space. When dealing with a massive geodesic in flat space, we can always transition to a reference frame where it is at rest. In Anti-de-Sitter space, the same principle applies. If we examine the oscillating path of a massive particle, we can "boost" to a frame where the particle is stationary. Consequently, the moving particle remains unaware of its motion, and contrary to appearances, there is no discernible "center" in Anti-de-Sitter space. The Hamiltonian is a component of the symmetry group, in similar fashion to the Poincare group, offering multiple options for a Hamiltonian. Once we select a specific Hamiltonian, such as the one responsible for shifting t in (3.1), we establish a "center" and a concept of the lowest energy state, often

represented by a particle situated at this designated "center".

In certain applications, it proves advantageous to concentrate on a small region of the boundary and treat it as $R^{1,d}$. In fact, there exists a choice of coordinates where the Anti-de-Sitter metric assumes the following form.

$$ds^2 = L^2 \frac{-dt^2 + d\vec{x}_{d-1}^2 + dz^2}{z^2} \tag{3.3}$$

in this metric, the boundary is positioned at $z = 0$, and we have slices that exhibit the Poincare symmetry group in d dimensions, one temporal and $d-1$ spatial dimensions. Interestingly, if we perform the transformation $t \to ix_0$, we arrive at hyperbolic space, which is occasionally referred to as Euclidean Anti-de-Sitter space! In these particular coordinates, we can also readily identify another isometry that scales the coordinates $(t, \vec{x}, z)$ as $(t, \vec{x}, z) \to \lambda(t, \vec{x}, z)$. These coordinate systems feature a horizon located at $z = \infty$ and cover only a segment of (3.1). These coordinates prove to be advantageous when we aim to explore a Conformal Field Theory (CFT) existing within Minkowski space, namely $R^{1,d-1}$.

The concept of the AdS/CFT correspondence postulates that all the physical phenomena within an asymptotically anti-de-Sitter spacetime can be effectively explained by a local quantum field theory existing on the spacetime's boundary, represented as $R \times S^{d-1}$. The symmetries of anti-de-Sitter space act upon this boundary, transforming points on the boundary into other points while preserving the boundary's structure. This action precisely mirrors the operations performed by the conformal group within d dimensions, which is $SO(2, d)$. Consequently, the quantum field theory is a conformal field theory. Remarkably, the rescaling symmetry described in equation (3.3) corresponds to a dilatation effect on the boundary. As a result, the boundary theory is scale invariant, without any dimensionful parameters. Typically, scale-invariant theories also possess conformal invariance, which has a stress-energy momentum tensor with a vanishing trace. The conformal group contains the Poincare group, dilatations, and "special conformal transformations", though the latter is of lesser significance here. Notably, the conformal symmetry allows us to select an arbitrary radius for the boundary S^{d-1}, which can be conveniently set to one. Additionally, in the context of a conformal field theory, the stress tensor's tracelessness implies that the field theory remains fundamentally unchanged

whether it operates on a space with a metric $g^b_{\mu\nu}$ or $\omega^2(x)g^b_{\mu\nu}$, with the understanding that this introduces a well-defined conformal anomaly. It's important to emphasize that we are referring to the metric on the boundary, where the field theory is situated, and this metric remains fixed and non-dynamical.

How can we reconcile the equivalence between a $d+1$-dimensional bulk theory and a d-dimensional one? Let's consider a skeptical viewpoint. If we count the number of degrees of freedom, it seems like there should be a contradiction due to the extra dimension in the bulk theory. Specifically, if we examine the number of degrees of freedom at high energies in the microcanonical ensemble, we can introduce an effective temperature. In a theory with massless fields or no characteristic scale, we anticipate that entropy scales as $S \sim V_{d-1}T^{d-1}$. Therefore, if the boundary theory is a conformal field theory (CFT) on $R \times S^3$, then for significantly high temperatures compared to the radius of S^3 ($T \gg 1$), we would expect the entropy to grow exponentially as

$$S \propto cT^{d-1} \tag{3.4}$$

where c is a dimensionless constant representing the effective count of fields within the theory. From a different perspective, the bulk theory appears to involve massless particles, such as gravitons. While there could be additional fields, for now, let's focus on the gravitons, which provide a lower limit for the entropy. The entropy associated with these gravitons is unquestionably greater than the entropy stemming from the region where r is approximately 1. Within this region, which has a volume of approximately one, we obtain

$$S_{\text{gas of gravitons}} > T^d \tag{3.5}$$

because it possesses d spatial dimensions. When T is sufficiently large, we observe that equation (3.5) surpasses equation (3.4). This seems to present a conflict with the fundamental premise of AdS/CFT. However, we are overlooking a crucial element: the presence of gravity within the bulk theory. Gravity leads to the emergence of black holes, and black holes impose limitations

on entropy. In AdS, black holes take the following form:

$$ds^2_{\mathrm{AdS_{d+1}}} = L^2\left[-(r^2+1-\frac{2gm}{r^{d-2}})dt^2+\frac{dr^2}{r^2+1-\frac{2gm}{r^{d-2}}}+r^2d\Omega^2_{d-1}\right] \tag{3.6}$$

where m is proportional to the mass and g is proportional to the Newton constant in units of the AdS radius

$$g \propto \frac{G_N^{d+1}}{L^{d-1}} \tag{3.7}$$

The gas of gravitons extends up to approximately $r_z \sim T$ and possesses a mass on the order of $m \sim T^{d+1}$. When T is sufficiently large, we can disregard the 1 in (3.6) when calculating the Schwarzschild radius: $r_s^d \sim gm \sim gT^{d+1}$. As a result, the Schwarzschild radius surpasses the system's size for sufficiently high temperatures, $T > 1/g$. Consequently, the calculation in (3.5) becomes invalid for such elevated temperatures. At elevated energies, we calculate the entropy based on black hole entropy, which expands in proportion to the horizon's area, $S \sim \frac{r_s^{d-1}}{g}$. It is worth noting that the Hawking temperature for sizable black holes follows $T \propto r_s$. The black hole's entropy can be expressed as $S_{BH} \sim \frac{1}{g}T^{d-1}$. This agrees with the anticipated form outlined in (3.4), with

$$c \propto \frac{1}{g} \propto \frac{L^{d-1}_{\mathrm{AdS}}}{G_{N,d+1}} \tag{3.8}$$

hence, AdS/CFT establishes a connection between the entropy of a black hole and the conventional thermal entropy of a field theory, yielding two significant implications. Firstly, it offers a statistical interpretation for black hole entropy, addressing conceptual issues surrounding black hole entropy. Furthermore, by representing black holes as ordinary thermal states within a unitary quantum field theory, it demonstrates the consistency of these black holes with quantum mechanics and unitary evolution. Secondly, it enables the calculation of thermal free energy and other thermal properties in quantum field theories with gravity duals.

The number of fields scales inversely with g in equation (3.8), which quantifies the effective gravitational coupling at the AdS scale. It represents the dimensionless constant measuring the effective nonlinear interactions among gravitons. Consequently, for a weakly coupled bulk theory, it is necessary for the field theory to possess a large number of fields. However, this is a

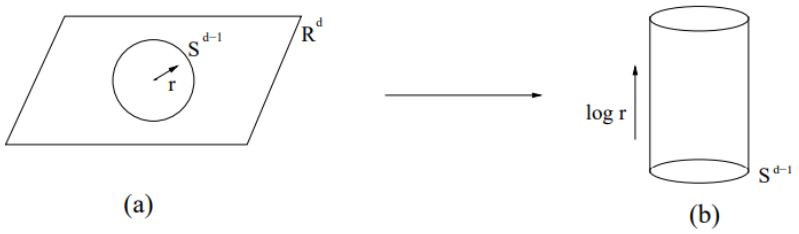

Figure 3.2: (a) In a conformal field theory defined on the Euclidean plane, R^d, we have the capability to apply various operators at the origin ($r = 0$). These operators generate specific states on S^{d-1} by executing the path integral of the field theory within the interior of S^{d-1} while the operators are inserted. (b) Thanks to the Weyl symmetry inherent to the theory, we can adjust the metric and reinterpret it as the metric for a cylindrical space, $R \times S^{d-1}$. States existing within this cylindrical context correspond one-to-one with operators residing on the plane. This characteristic is a fundamental attribute of conformal field theories and is entirely unrelated to the concept of AdS/CFT. (Image credits: [48])

necessary but not sufficient condition. An essential characteristic of a weakly coupled theory is the presence of a Fock space structure within the Hilbert space. This structure facilitates discussions about single particles, two particles, and so on, with their energies being proportional to the sum of the energies of individual particles with minor corrections. The dual quantum field theory must exhibit a similar structural property. Large N gauge theories naturally exhibit this structure. A large N gauge theory, based on the $SU(N)$ or $U(N)$ gauge group with fields in the adjoint representation, allows the formation of gauge-invariant operators by taking traces of fundamental fields, such as $\mathrm{Tr}[F_{\mu\nu}F^{\mu\nu}]$ or $\mathrm{Tr}[F_{\mu\nu}D_\rho D_\sigma F^{\mu\nu}]$, all of which are local operators evaluated at the same spacetime point. Additionally, double trace operators, representing the product of two operators, can be considered. Such operators create a state when they act on the field theory vacuum. In a general CFT, even without a known gravity dual, there exists a correspondence between states on the cylinder, $R \times S^{d-1}$, and operators on the plane, R^d. The dimension of the operator corresponds to the energy of the associated state, where the scaling dimension indicates how the operator transforms under scaling transformations mentioned after (3.3). This correspondence arises when we consider an Euclidean cylinder, where the Euclidean cylinder and the plane differ only by an overall Weyl transformation of the metric, $d(\log r)^2 + d\Omega^2 = \frac{1}{r^2}[dr^2 + r^2 d\Omega^2]$, resulting in them being equivalent in a CFT. An operator located at the origin of the plane generates a state at a fixed r, which can be interpreted as a state in the field theory on the cylinder (refer to figure 3.2). This state-operator mapping

applies to any conformal field theory.

AdS/CFT establishes a connection between a state in the field theory on the cylinder and a state in the bulk theory in global coordinates (3.1), as both sides share the same symmetries. States or operators can be categorized based on their transformation properties under the conformal group, characterized by the operator's spin and scaling dimension, Δ. For instance, the stress tensor operator, $T_{\mu\nu}$, generates a graviton in AdS, with the dimension of the stress tensor being d. Single trace operators are associated with single-particle states in the bulk, while multitrace operators correspond to multiparticle states in the bulk. A general argument, derived from a straightforward analysis of Feynman diagrams, indicates that the dimensions of multitrace operators are the sum of the dimensions of each single trace component, subject to $1/N^2$ corrections. Remarkably, the same analysis of Feynman diagrams reveals that the large N limit of general gauge theories leads to a string theory [77]. The argument doesn't specify the exact type of string theory it implies; it simply suggests that we can organize the diagrams into those that can be drawn on a sphere, plus those on the torus, and so on. As we increase the genus of the surface, we introduce an additional factor of $1/N^2$. This resembles a string theory with a string coupling parameter, g_s, roughly proportional to $1/N$. Importantly, the strings present in the bulk align with the strings implied by this reasoning.

The preceding argument emphasizes that the large N limit is essential for achieving a weakly coupled gravity theory. However, this doesn't imply that we are confined to linearized solutions. In a weakly coupled gravity theory, we can explore complete classical nonlinear solutions of the equations, such as the black hole solutions mentioned earlier. Weak coupling implies that we can disregard quantum gravity corrections or loop diagrams.

In string theory, the graviton represents the lowest oscillation mode of a string. The gravitational coupling discussed earlier relates to the strength of interactions between strings. Nonetheless, there is an additional requirement for the validity of the gravity approximation. In gravity, we treat the graviton as a point-like particle while disregarding all the massive string states. The typical size of the graviton corresponds to the string length, l_s, which is an extra parameter beyond the Planck scale. To neglect the influence of the remaining string states, we require

that

$$\frac{L_{\text{AdS}}}{l_s} \gg 1, \text{for gravity to be a good approximation} \tag{3.9}$$

This condition can be simplified as ensuring that the typical spatial scale is significantly larger than the inherent size of the graviton in string theory. Emphasizing its importance, this condition must be satisfied in numerous practical instances to prevent gravity from yielding incorrect results, even when dealing with a substantial number of fields. If equation (3.9) does not hold true, then we must take into account the complete string theory within AdS. A notable characteristic of string theory is the presence of massive string states with spins greater than 2. In large N gauge theories, we can readily construct single-trace operators featuring higher spins, such as $\text{Tr}[F_{\mu\nu}D_+^S F^{\mu\nu}]$, where D_+ represents a derivative along a null direction. These operators possess relatively modest scaling dimensions at weak coupling, typically $\Delta = 4 + S$. Consequently, they give rise to particles with spin S, whose bulk mass is of similar magnitude to the inverse AdS radius. The presence of such lightweight string states invalidates the Einstein gravity approximation. Therefore, for the gravity approximation to be reliable, the field theory must exhibit strong interactions. This is a necessary condition, although not sufficient on its own. The coupling must be powerful enough to give considerable dimensions to all the single-trace operators with higher spins within the theory. In specific instances, we discover that this quantity, (3.9), is directly proportional to a positive exponent of the effective 't Hooft coupling of the theory, denoted as $g_{\text{YM}}^2 N$. Where g_{YM} is the coupling constant of the gauge theory and the additional factor of N arises from the exchange of N gluons among color-correlated particles, which amplifies their interactions in the context of large N By selecting a sizable value for $g_{\text{YM}}^2 N$, we can give significant dimensions to the higher spin states, leaving us with a lightweight graviton and other lower spin states. In such cases, we anticipate that their interactions align with those of Einstein gravity.

3.1.2 An example: $N = 4$ Super Yang Mills

The preceding discussion presented a quite general overview. To get into specifics, we will explore a particular example of a dual pair. We will commence with a discussion of the field

theory, followed by an examination of the gravity theory. Throughout this exploration, we will illustrate how various elements align between the two domains.

We direct our attention to a four-dimensional field theory that bears resemblance to quantum chromodynamics. In quantum chromodynamics, we encounter a gauge field,A_μ, which constitutes a traceless 3×3 matrix within the adjoint representation of $SU(3)$. The corresponding action is defined as follows

$$\begin{aligned} S &= -\frac{1}{4g_{\mathrm{YM}}^2}\int d^4x \mathrm{Tr}[F_{\mu\nu}F^{\mu\nu}] \\ F_{\mu\nu} &= [\partial_\mu + A_\mu, \partial_\nu + A_\nu] \end{aligned} \tag{3.10}$$

We can extend this theory by considering a gauge group $SU(N)$ or $U(N)$, where A_μ is now represented as an $N \times N$ matrix. In the case of quantum chromodynamics (QCD), fermions in the fundamental representation are present. However, in this scenario, we adopt a different approach by introducing fermions that transform within the adjoint representation. The rationale behind this choice is our desire to construct a supersymmetric theory. Supersymmetry serves as a valuable tool for validating many of the predictions arising from the duality. While the existence of the duality does not hinge on supersymmetry, finding a dual pair becomes more manageable in its presence. Supersymmetry is a symmetry that establishes a relationship between bosons and fermions. In a supersymmetric theory, both the bosons and their fermionic counterparts belong to the same representation of the gauge group. By introducing a Majorana fermion in the adjoint representation, we obtain an $N = 1$ supersymmetric theory. It's important to note that this theory lacks quantum conformal symmetry and exhibits a beta function, similar to the theory with no fermions. Conversely, if we include four fermions denoted as χ_α and six scalars labeled as ϕ^I, all residing in the adjoint representation and have specific couplings, we create a theory endowed with maximal supersymmetry known as $N = 4$ supersymmetric theory [28]. The Lagrangian of this theory is entirely determined by supersymmetry and the choice of the gauge group. The action has the schematic form

$$S = -\frac{1}{4g_{\mathrm{YM}}^2}\int d^4x \mathrm{Tr}\left[F^2 + 2(D_\mu\phi^I)^2 + \chi D\chi + \chi[\phi,\chi] - \sum_{IJ}[\phi^I,\phi^J]^2\right] + \frac{\theta}{8\pi^2}\int \mathrm{Tr}[F\wedge F] \tag{3.11}$$

there exist two crucial constants: the coupling constant,$g^2_{\rm YM}$, and the θ angle. Supersymmetry dictates all the relative coefficients in the Lagrangian. All fields are in a single supermultiplet under supersymmetry. Remarkably, this theory demonstrates both classical and quantum conformal invariance, signifying that its beta function equals zero. In simpler terms, it retains its coupling strength irrespective of energy scales. Once the coupling strength is determined, it remains constant across all energy levels. Whether it is weak or strong, this characteristic persists. The effective coupling constant is

$$\lambda = g^2_{\rm YM} N \tag{3.12}$$

the additional factor of N can be explained as follows: when two fields have their color and anticolor entangled or summed over, there are N gluons that can be exchanged between them while preserving this entanglement. The theory possesses an $SO(6)$, or $SU(4)$, R-symmetry that rotates the six scalars and the fermions. An R-symmetry is a type of symmetry that does not commute with supersymmetry, which is the case here because bosons and fermions belong to different representations of $SU(4)$.

Now, let's get into the gravity theory, which is a string theory giving rise to a quantum mechanically consistent theory of gravity. Since we began with a supersymmetric gauge theory, we also anticipate a supersymmetric string theory. Ten-dimensional supersymmetric string theories are well-established, with one such theory, type IIB, consisting solely of closed oriented strings. At long distances, this string theory reduces to a gravity theory known as type IIB supergravity[67]. This supergravity theory encompasses the metric and other massless fields mandated by supersymmetry, including a five-form field strength denoted as $F_{\mu 1 \ldots \mu 5}$, which is entirely antisymmetric in its indices. Additionally, it is constrained to be self-dual ($F_5 = *F_5$), analogous to the two-form field strength $F_{\mu\nu}$ in electromagnetism. In four dimensions, charged black hole solutions can incorporate the metric and the electric or magnetic two-form field strength. Particularly, the near-horizon solution of an extremal black hole exhibits $AdS_2 \times S^2$ geometry with a two-form flux on the AdS_2 or the S^2, depending on whether it is electrically or magnetically charged. A similar phenomenon arises in ten dimensions. There exist a solution

to the equations that takes the shape of $AdS_5 \times S^5$, featuring a five-form field along both the AdS_5 and S^5 directions. This configuration has both electric and magnetic fields, which is a result of the self-duality constraint on F_5. According to the Dirac quantization condition, magnetic fluxes on an S^2 are quantized. In the context of string theory, the flux on the S^5 is also quantized

$$\int_{S^5} F_5 \propto N \tag{3.13}$$

which is the same number of colors of the gauge theory. In ten dimensional supergravity, the relevant equations of motions follow the action

$$S = \frac{1}{(2\pi)^7 l_p^8} \int d^{10}x \sqrt{g}(R - F_5^2) \tag{3.14}$$

in addition to the self duality constraint, $F_5 = *F_5$. The equations of motion establish a connection between the radii of AdS_5 and S^5 with respect to N. Specifically, we find that both radii are determined by $\frac{L^4}{l_p^4} = 4\pi N$, where l_p is the Planck length. In the context of string theory, we also have the string length $l_s = g_s^{-1/4} l_p$, which sets the string tension $T = 1/(2\pi l_s^2)$. Here, g_s represents the string coupling determining the interaction strength between strings and is derived from the vacuum expectation value of one of the ten-dimensional theory's massless fields, $g_s = \langle e^{\phi} \rangle$. In the gravity theory, there is an additional massless scalar field χ, which acts as an axion with a periodicity of $\chi \to \chi + 2\pi$. These two fields are associated with the parameters g^2_{YM} and θ present in the aforementioned Lagrangian. It is natural to identify θ with the boundary condition or expectation value for χ and g^2_{YM} with the string coupling g_s.Namely, $g^2_{\mathrm{YM}} = 4\pi g_s$. The precise numerical coefficient can be determined through the physics of D-branes [60] or by applying the S-duality of both theories. Once this is done, we can express the radii of AdS_5 and S^5 in terms of Yang-Mills quantities

$$\begin{aligned} \frac{L^4}{l_s^4} &= 4\pi g_s N = g^2_{\mathrm{YM}} N = \lambda \\ \frac{L^4}{l_p^4} &= 4\pi N \end{aligned} \tag{3.15}$$

As we previously explained, to ensure a weakly coupled bulk theory, it is essential that $N \gg$

1. Furthermore, for the Einstein gravity approximation to be reliable, a substantial effective coupling is required. Consequently, we find ourselves in the following scenarios:
$g^2_{\rm YM} \gg 1$: Gravity is good, gauge theory is strongly coupled
$g^2_{\rm YM} \ll 1$: Gravity is not good, gauge theory is weakly coupled
under such extreme regimes, it is easy to do computations using one of the two descriptions.

The 't Hooft limit [77], which deals with planar diagrams, corresponds to taking $N \to \infty$ while keeping $g^2_{\rm YM}N$fixed. It can be advantageous to first approach the 't Hooft limit, resulting in a free string theory in the bulk, and then vary the 't Hooft coupling λ from weak to strong. This variation changes the AdS radius in string units. The behavior of the string is dictated by a two-dimensional field theory with AdS as its target space (along with S^5 and some fermionic dimensions). This two-dimensional field theory is weakly coupled when the AdS radius is large and strongly coupled when the radius is small, or when the gauge theory is weakly coupled. When dealing with values of order one, $g^2_{\rm YM}N \sim 1$, one must utilize the full string theory description or solve the complete planar gauge theory.

$N = 4$ super Yang-Mills theory possesses an S-duality symmetry, which interchangeably relates weak and strong coupling regimes. One might be tempted to transition to a strong coupling regime and then employ S-duality to return to a weakly coupled theory. However, this approach is not effective. The bulk theory also exhibits an S-duality symmetry, and these two S-duality symmetries are in a one-to-one correspondence. Therefore, to assess the validity of the gravity description, we first apply S-duality on both sides to set $g_s < 1$ and subsequently employ the aforementioned criterion.

It is worth revisiting the problem of comparing the thermal free energy of the gauge theory and the gravity theory while considering numerical coefficients. We examine the field theory in

$R^3 \times S^1_\beta$. The free energy at weak coupling is given by the formula:

$$\begin{aligned} -\beta F &= V \int \frac{d^3k}{(2\pi)^3} \left[n_{\text{bosons}} \log(\frac{1}{1-e^{-\beta|\vec{k}|}}) + n_{\text{fermions}} \log(1+e^{-\beta|\vec{k}|}) \right] \\ -\beta F &= \frac{\pi^2}{6} V N^2 T^3 \\ \beta &= 1/T \end{aligned} \tag{3.16}$$

where we used $n_{\text{bosons}} = n_{\text{fermions}} = 8N^2$. At strong coupling, we take the Euclidean black brane solution with $\tau \sim \tau + \beta$

$$ds^2 = L^2 \left[(1 - \frac{z^4}{z_0^4}) \frac{d\tau^2}{z^2} + \frac{dz^2}{z^2(1-\frac{z^4}{z_0^4})} + \frac{dx^2}{z^2} \right] \tag{3.17}$$

this is straightforwardly connected to the limit of large mass in equation (3.6). By requiring the absence of a singularity at $z = z_0$, we can establish the relationship $\beta = \pi z_0$, as usual. The entropy is determined by the familiar Bekenstein-Hawking formula [31]

$$S = \frac{\text{Area}}{4G_N} = \frac{L^8 V_{S^5}}{4G_{N,10} z_0^3} = \frac{\pi^2}{2} V N^2 T^3 \tag{3.18}$$

computing the free energy from the entropy, we get

$$-\beta F = S/4 = \frac{\pi^2}{8} V N^2 T^3 \tag{3.19}$$

We observe that there exists a 3/4 factor difference between equations (3.19) and (3.16). This doesn't signify a contradiction with AdS/CFT; instead, it provides a prediction for how the free energy varies when transitioning from weak to strong coupling. In line with general large N principles, we anticipate the free energy to exhibit the following structure

$$\frac{F(\lambda, N)}{F(\lambda = 0, N)} = f_0(\lambda) + \frac{1}{N^2} f_1(\lambda) + \dots \tag{3.20}$$

We anticipate that the function $f_0(\lambda)$ exhibits a smooth transition from $f_0 = 1$ at $\lambda = 0$ to $f_0 = 3/4$ at $\lambda \gg 1$. Indeed, the leading corrections from both of these values have been

calculated, and they align with our initial expectations [32, 23]. In this specific case, the function f_0 remains constant at large λ. However, there are instances where this function behaves as $f_0 \sim \sqrt{1/\lambda}$ for large λ [1, 21].

Within the gauge theory, there exist scalar fields with potential energy landscapes that feature flat directions. This allows for the possibility of assigning expectation values to these fields while having the vacuum energy fixed at zero, resulting in the spontaneous breaking of conformal symmetry. While the conformal symmetry is restored at high energies, it remains broken at lower energy scales. These flat directions correspond to diagonal matrices as expectation values for the scalar fields. As a straightforward example, we can set $\phi^1 = \text{diag}(a, 0, \ldots, 0)$, with all the other components being zero. This breaks the gauge group from $U(N)$ to $U(1)\times U(N-1)$. In the context of the gravity dual, this corresponds to placing a D3 brane at a position approximately $z \sim 1/a$ in the Poincare coordinates (3.3). Intuitively, one might expect that gravitational forces would push the brane toward the horizon. However, this force is exactly counteracted by an electric repulsion stemming from the presence of the electric five-form field strength. The massless fields associated with this D3 brane are linked to the fields within the $U(1)$ factor, while the massive W bosons arising from the Higgs mechanism originates from strings extending from the brane to the horizon. Interestingly, it is possible to formulate solutions corresponding to general vacuum expectation values

$$\begin{aligned} ds^2 &= f^{-1/2}(-dt^2 + d\vec{x}^2) + f^{1/2}(d\vec{y}^2) \\ f &= 4\pi \sum_i \frac{l_p^4}{|\vec{y} - \vec{y}_i|^4} \end{aligned} \tag{3.21}$$

in this expression, $\vec{x}$ represents a three-dimensional vector, while $\vec{y}$ is a six-dimensional vector. The $\vec{y}_i$ are associated with the vacuum expectation values of the scalar fields, $\vec{\phi} = \text{diag}(\vec{y}_1, \vec{y}_2, \ldots, \vec{y}_N)$. This solution resembles a black brane with multiple centers. In principle, we cannot rely on this solution in the vicinity of a single center due to the extremely high curvature. However, when multiple centers coincide, we can trust the solution. For instance, if we break $U(2N) \to U(N) \times U(N)$ by assigning the expectation value $\phi^1 = \text{diag}(a, \ldots, a, 0, \ldots, 0)$, with a repeated N times, this solution remains reliable across all regions. In the ultraviolet

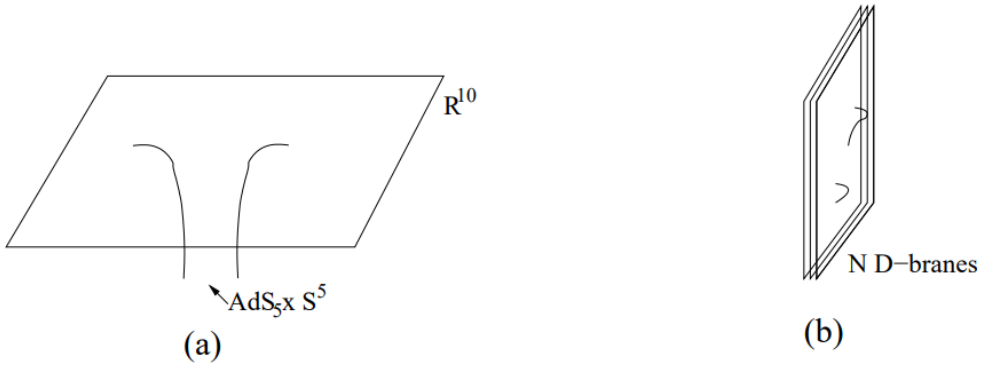

Figure 3.3: (a) The structure of the black 3-brane solution (3.21) with (3.22) results in a specific geometry. In the distant region, we have ten-dimensional flat space. As we approach the vicinity of the horizon, the geometry transforms into $AdS_5 \times S^5$. (b) Describing D-branes involves understanding their excitations, which are illustrated by open strings residing on these branes. These strings can begin and end on any of the N D-branes, giving us a total of N^2 strings. In the low-energy regime, these excitations lead to the emergence of a $U(N)$ gauge theory known as $N = 4$ super Yang-Mills. (Image credits: [48])

(UV), for large $|\vec{y}|$, we have a single AdS geometry that splits into two AdS throats with smaller radii as we progress toward lower values of $|\vec{y}|$. This describes the corresponding transition in the gauge theory from the UV to the infrared (IR), where we encounter two decoupled conformal field theories. This example illustrates a geometry that is solely asymptotically AdS near the boundary but displays differences within the interior.

It is interesting to consider the solution (3.21) with [39]

$$f = 1 + \frac{4\pi N l_p^4}{|y|^4} \tag{3.22}$$

this provides a physical basis for deriving the gauge-gravity duality in this specific example [47]. The solution becomes ten-dimensional flat space for $|\vec{y}| \gg N^{1/4} l_p$. It represents an extremal black D3 brane, as illustrated in figure 3.3. This brane spans $1 + 3$ dimensions of spacetime, denoted as t and $\vec{x}$, while it localizes in six additional dimensions represented by $\vec{y}$. Transitioning to the near-horizon regime of this black D3 brane is done by taking y to small values and omitting the 1 in (3.22). In cases where the string coupling is very small, $g_s N \ll 1$, this system can be described as a set of N D3 branes. D3 branes are solitonic defects present in string theory [59]. They are characterized by a simple string theory construction, revealing

that they yield $N = 4$ super Yang-Mills theory at low energies.

Understanding the scalar fields is relatively straightforward: they originate from the motion of the branes in the six transverse dimensions. Regarding the gauge fields, they emerge from supersymmetry. Although a system of N identical branes typically exhibits an ordinary S_N permutation symmetry, for these branes, this symmetry extends to form a complete $U(N)$ gauge symmetry. As such, we have two descriptions of the brane: firstly, as a black brane, and secondly, as a collection of D-branes. Now, we can approach the low-energy limit for each of these descriptions. The low-energy limit of the D-branes leads to the $N = 4U(N)$ super Yang-Mills theory. Conversely, the low-energy limit on the gravity side corresponds to approaching the vicinity of the black D3 brane's horizon. In this region, the substantial redshift factor, where $f^{-1/2} \to 0$, results in very low energy to all particles residing within this near-horizon zone. This region essentially corresponds to $AdS_5 \times S^5$. Assuming the equivalence of these two descriptions, we have achieved the gauge-gravity duality.

3.2 BFSS model

In this section we are going to discuss the BFSS[1] model [3], which was proposed as the first nonperturbative formulation of a quantum theory that includes gravity. The lagrangian used for this model is,

$$L = \frac{1}{2g}[\mathrm{tr}\dot{X}^i\dot{X}^i + 2\theta^T\dot{\theta} - \frac{1}{2}\mathrm{tr}[X^i, X^j]^2 - 2\theta^T\gamma_i[\theta, X^i]] \tag{3.23}$$

This is a quantum mechanical theory, where g is the coupling constant, X represent nine $N \times N$ matrices, $X^i_{a,b}$ with $i = \{1, \ldots, 9\}$ and $a, b = \{1, \ldots, N\}$, connected with 16 fermionic superpartners $\theta_{a,b}$ which transform as spinors under $SO(9)$, γ_i are gamma matrices. This lagrangian (3.23) has a $U(N)$ gauge symmetry. We can always fix the gauge, so that $A = 0$, as done here.

It is worth noting that the same lagrangian was used before by [20] to study some properties of

[1] Named after: T. Banks, W. Fischler, S.H. Shenker and L. Susskind.

weakly coupled string theory. In that paper, The 11-D Planck length scale emerged naturally as the dynamical length scale. This together with the fact that there was some evidence for the large N limit of the quantum theory defined by (3.23) to be indeed Lorentz invariant motivated the idea of using it as the basis for this model.

It is more convenient to rewrite (3.23) in units where the 11-D Planck length is 1.

$$L = \mathrm{tr}\left[\frac{1}{2R}D_tY^iD_tY^i - \frac{1}{4}R[Y^i,Y^j]^2 - \theta^TD_t\theta - R\theta^T\gamma_i[\theta,Y^i]\right] \tag{3.24}$$

In here, R is called the compactification radius which is related to the coupling constant by $R = gl_s$ where l_s is the length scale[2], $Y = \frac{X}{g^{1/3}}$, and the gauge field is no longer fixed, so that $D_t = \partial_t + iA$. The SUSY transformation laws for (3.24) are,

$$\delta X^i = -2\epsilon^T\gamma^i\theta \tag{3.25}$$

$$\delta\theta = \frac{1}{2}\Big[D_tX^i\gamma_i + \gamma_- + \frac{1}{2}[X^i,X^j]\gamma_{ij}\Big]\epsilon + \epsilon^{'} \tag{3.26}$$

$$\delta A = -2\epsilon^T\theta \tag{3.27}$$

From this we get the Hamiltonian[3],

$$H = R\,\mathrm{tr}\left\{\frac{\Pi_i\Pi_i}{2} + \frac{1}{4}[Y^i,Y^j]^2 + \theta^T\gamma_i[\theta,Y^i]\right\} \tag{3.28}$$

In which Π is the canonical conjugate to Y.

3.2.1 Moving to large N

Although it was believed that large N gauge theories (i.e. QFT theories) have a string theory (i.e. gravity) description [77]. The methodology for achieving this feat was not quite understood in [3]. To do this properly one must follow the work done in [41] keeping in mind that BFSS is

[2] In (3.24) this was set to 1

[3] The epsilons ϵ & $\epsilon^{'}$ in (3.26) are two independent 16 component anticommuting SUSY parameters

a D0 Brane model. It is of great importance to understand why we are interested only in the large N limit. To explain it simply, it is known that D-branes carry mass and charge, hence they excite the bulk gravity modes and one can find supergravity solutions with the same mass and charge. This might seem wrong at first glance because supergravity solutions describe exclusively the long range fields of the D-branes, since supergravity is not expected to be valid at short distances. However, General Covariance says that supergravity solutions are validated as long as curvatures are locally small compared to the string scale (i.e. the Planck scale). For a system with large number of branes (i.e. large N) the curvatures are small and hence the supergravity solutions are valid even at small distance scale. The supergravity solution (i.e. string theory) for this model is,

$$ds^2 = \alpha^{'}\left(-\frac{U^{7/2}}{4\pi^2 g\sqrt{15\pi N}}dt^2 + \frac{4\pi^2 g\sqrt{15\pi N}}{U^{7/2}}dU^2 + \frac{4\pi^2 g\sqrt{15\pi N}}{U^{3/2}}d\Omega^2\right) \tag{3.29}$$

$$e^{\phi} = 4\pi^2 g^2\left(\frac{240\pi^5 g^2 N}{U^7}\right)^{3/4} \tag{3.30}$$

to achieve the aforementioned conditions, we take the field theory limit

$$U \equiv \frac{r}{\alpha^{'}} = \text{fixed},\ \ g^2 = \frac{1}{4\pi^2}\frac{g_s}{\alpha^{'3/2}} = \text{fixed},\ \ \alpha^{'} \to 0. \tag{3.31}$$

where U is an energy coordinate, r is the radial coordinate in flat space of d-branes, $\alpha^{'}$ is the string tension, g_s is the string coupling. Note that $g_s = e^{\phi_\infty}$ where ϕ is called the dilaton in string theory and ϕ_∞ is the value very far away from the d-branes.
The effictive dimensionless coupling constant is $g^2_{eff} \approx g^2 N U^{p-3}$. Hence for D0 branes, or in other words $p = 0$, our calculations are trusted in the high energy region $g_{eff} \ll 1$ which gives $U > g^{2/3}N^{1/3}$.

The effective string coupling and curvature are small when,

$$g^{2/3}N^{1/7} \ll U \ll g^{2/3}N^{1/3} \tag{3.32}$$

hence, the type IIA description is valid in this region.

Now, let us study the low energy region. To do this, we may uplift the solution to eleven dimensions. This is done by taking an uncharged black string along x_{11} and then boosting it along x_{11} while taking the limit,

$$\gamma \to \infty, \quad \gamma\mu = \frac{N}{2\pi R_{11}^2} = \text{fixed} \tag{3.33}$$

where μ is the mass per unit length of the black string in its rest frame. As shown by [37] this solution can not be trusted in regions where

$$U_0 \sim g^{2/3} N^{1/9} \tag{3.34}$$

For $U_0 \ll g^{2/3} N^{1/9}$ we get a Schwarschild black hole boosted along the eleventh direction. The radius of the black hole in Planck units is given by,

$$(\frac{r_s}{l_p})^8 \sim \frac{E^{1/2} N^{1/2}}{g^1/3} \sim \frac{U_0^{7/2} N^{1/2}}{g^{7/3}} \tag{3.35}$$

So the gravity description is trusted where $U_0 \gg g^{2/3} N^{-1/7}$. For lower energies the system is expected to behave as a single graviton.

Lattice simulations can be done on this model, as seen in [43, 22, 11, 10]

3.3 BMN model

BMN[4] is a matrix model associated to the M-theory pp-wave background[9]. The M-theory metric is

$$\begin{aligned} ds^2 &= -4dx^- dx^+ - [(\frac{\mu}{3})^2 (x_1^2 + x_2^2 + x_3^2) + (\frac{\mu}{6})^2 (x_4^2 + \cdots + x_9^2)] dx^{+^2} + d\vec{x}^2 \\ F_{+123} &= \mu \end{aligned} \tag{3.36}$$

[4] Named after: David Berenstein, Juan Maldacena and Horatiu Nastase.

In similar fashion to [3, 76, 71, 68] we take $x^- \sim x^- + 2\pi R$, and $2p^+ = -p_- = N/R$.

Having done this, the dynamics of this theory can be given by the matrix model with the action

$$\begin{aligned} S &= S_{\text{BFSS}} + S_{\text{mass}} \\ S_{BFSS} &= \int dt \text{Tr}\left[\sum_{j=1}^{9} \frac{1}{2(2R)}(D_0\phi^j)^2 + \Psi^T D_0 \Psi + \frac{(2R)}{4}\sum_{j,k=1}^{9}[\phi^j,\phi^k]^2 + \sum_{j=1}^{9} i(2R)(\Psi^T\gamma^i[\Psi,\phi^j])\right] \\ S_{\text{mass}} &= \int dt \text{Tr}\left[\frac{1}{2(2R)}\left(-(\frac{\mu}{3})^2\sum_{j=1,2,3}(\phi^j)^2 - (\frac{\mu}{6})^2\sum_{j=4}^{9}(\phi^j)^2\right) - \frac{\mu}{4}\Psi^T\gamma_{123}\Psi - \frac{\mu}{3}i\sum_{j,k,l=1}^{3}\text{Tr}(\phi^j\phi^k\phi^l)\epsilon_{jkl}\right] \end{aligned} \tag{3.37}$$

Where l_p is set to 1. Note that $t = x^+$ and $\phi = \frac{r}{2\pi}$ where r is the physical distance in eleven dimensions, and $\gamma_{123} = \gamma_1\gamma_2\gamma_3$. S_{BFSS} is the action of the BFSS model written in Maldacena's notation, comparing (3.37) to (3.24) we see that indeed ϕ is Y and Ψ is θ, with minor differences due to conventions. Namely, $2R_{\text{EQ3.15}} = R_{\text{EQ3.2}}$ and l_p is normalized such that $\sqrt{\alpha'} = l_p g^{-1/3}$. S_{mass} breaks the symmetry $SO(9) \to SO(6) \times SO(3)$ and gives mass to the scalar and fermion fields, it also adds a Myers effect term[54].

3.3.1 How BMN is different compared to BFSS

This model (3.37) has the SUSY transformation rules,

$$\begin{aligned} \delta\phi^i &= \Psi^T\gamma^i\epsilon(t) \\ \delta\Psi &= \left(\frac{1}{(2R)}D_0\phi^i\gamma^i + \frac{\mu}{6(2R)}\sum_{i=1}^{3}\phi^i\gamma^i\gamma_{123} - \frac{\mu}{3(2R)}\sum_{i=4}^{9}\phi^i\gamma^i\gamma_{123} + \frac{i}{2}[\phi^i,\phi^j]\gamma_{ij}\right) \\ \delta A_0 &= \Psi^T\epsilon(t) \\ \epsilon(t) &= e^{-\frac{\mu}{12}\gamma_{123}t}\epsilon_0 \end{aligned} \tag{3.38}$$

Imposing $\delta\Psi = 0$ we find the solutions [5]

$$[\phi^i,\phi^j] = i\frac{\mu}{6R}\epsilon_{ijk}\phi^k \quad i,j,k = 1,2,3 \quad \dot{\phi}^i = 0 \text{ for all } \quad i \quad \text{and } \phi^i = 0 \text{ for } i = 4,\ldots,9 \tag{3.39}$$

[5] This condition is imposed to get the fully supersymmetric solutions of (3.37)

From this, we see that the number of solutions is discrete. Hence, solving the full quantum mechanical problem of the ground state wavefunction is not needed. In contrast to BFSS, which had the issue of having to undergo such tiresome calculation.

Thermodynamic simulation of the BMN model has been done in [19], as well as lattice analysis [17, 2, 66].

3.4 Ungauged model

The ungauged model [50] is a variant of the BFSS model, in which we treat the $SU(N)$ symmetry as being global instead of gauging it. To illustrate how this is done, consider the BFSS action

$$S = \frac{1}{g^2}\int dt \mathrm{Tr}\left(\frac{1}{2}(D_t X^I)^2 + \frac{1}{2}\psi_\alpha D_t \psi_\alpha + \frac{1}{4}[X^I, X^J]^2 + \frac{1}{2} i\psi_\alpha \gamma^I_{\alpha\beta}[\psi_\beta, X^I]\right) \tag{3.40}$$

Where the covariant derivative is defined as $D_t B = \partial_t B + i[A_t, B]$ and A_t is the gauge field. To treat the $SU(N)$ symmetry as a global symmetry, we simply set $A_t = 0$ in (3.40). The resulting theory has a singlet subsector identical to the original one, but it introduces non-singlet states.

3.4.1 Supersymmetric properties of the ungauged model

First, we would like to know whether setting $A_t = 0$ alters the supersymmetric properties. We have the Q_a operators that were generating the SUSY transformation in the original theory

$$Q\epsilon = -\frac{1}{g^2}\mathrm{Tr}\left(\dot{X}^I \psi \gamma^I \epsilon + i\frac{1}{2}[X^K, X^L]\psi\gamma^{KL}\epsilon\right) \tag{3.41}$$

Where $\gamma^{KL} = \frac{1}{2}(\gamma^K\gamma^L - \gamma^L\gamma^K)$. We would like to know if these operators commute with the resulting hamiltonian[6]

$$[Q_a, H] = -\mathrm{Tr}(\psi_a G) \tag{3.42}$$

[6] The resulting hamiltonian is the usual hamiltonian we get from (3.40) with A_t set to zero

Where G is the $SU(N)$ symmetry generators.[7] From this we see that (3.42) vanishes in singlet states, but does not on non-singlet states. Hence, the non-singlet states are not supersymmetry multiplets. Furthermore, computing the anticommutators

$$\{Q_\alpha, Q_\beta\} = 2H\delta_{\alpha\beta} + 2\mathrm{Tr}(GX^I)\gamma^I_{\alpha\beta} \tag{3.43}$$

In the ungauged model we get a non-zero right hand side. This is because the supersymmetry tranformation only close up to $SU(N)$ transformations, which are gauge transformations. However, we can still extract some useful information from this algebra. Namely, we can deduce that non-singlet states, as well as singlet states, have non-negitave energy. Recalling that the supercharges are are self-adjoin $Q^\dagger_\alpha = Q_\alpha$ and gamma matrices are traceless, one can sum over the spinorial indices to get

$$32H = \sum_{\alpha=1}^{16}\{Q_\alpha, Q_\alpha\} = \sum_{\alpha=1}^{16}\{Q^\dagger_\alpha, Q_\alpha\} \geq 0 \tag{3.44}$$

We could redefine the Hamiltonian to preserve some of the supersymmetry.

$$H_{\mathrm{SUSY}} = H - \mathrm{Tr}(X^1 G) \tag{3.45}$$

By doing this, we break the $SO(9)$ symmetry to $SO(8)$ but preserve half of the supersymmetry, namely those whose spinorial parameter obeys

$$(\gamma^1 + \mathbf{1})\epsilon = 0 \tag{3.46}$$

We also recover the standard SUSY algebra

$$\{Q\cdot\epsilon, Q\cdot\epsilon^{'}\} = 2H_{\mathrm{SUSY}}\epsilon\cdot\epsilon^{'} \tag{3.47}$$

[7] $G = \frac{i}{2g^2}(2[D_t X^I, X^I] + [\psi_\alpha, \psi_\alpha])$

3.4.2 Similarities with the original model

Although we have been examining the differences between the original (i.e gauged) and the resulting (i.e ungauged) model, they can be much more similar. To see this, consider the original theory with an additional external quark in some representation $\bar{R}$. The simplest way to achieve this is by adding the operator $\mathrm{Tr}_{\bar{R}} P e^{i\int A_t dt}$ which completely breaks the supersymmetery. Alternatively, the operator[8] of the form $\mathrm{Tr}_{\bar{R}} P e^{i\int dt(A_t + X^1)}$ preserves half of the supersymmetries [46, 65], this corresponds to the Hamiltonian (3.45). Hence, the ungauged model is similar to the original model with these operators inserted in.

Another important point is that the BFSS model was introduced with the specific purpose of deriving the S-matrix for 11-dimensional M-theory. The BFSS proposal focuses on a highly restricted energy regime within this matrix model. In this extremely low-energy limit, we delve deep into the bulk region, where the 11th dimension becomes significantly larger in scale compared to other relevant quantities. In this regime, the physical behavior is anticipated to faithfully reproduce that of the full 11-dimensional theory. It appears that the distinction between the gauged and ungauged models becomes indistinct as we approach such low energies, where the energy E scales inversely with the number of degrees of freedom N ($E \propto 1/N$). Hence, the ungauged model is as good as the gauged one in this low-energy regime.

3.5 The simplest model yet

We have discussed three important models: BFSS, BMN and the ungauged model. Although each model was simpler than the one before it to some extent, they all involve quantum field theory. In this section, we will discuss a system built fully by ordinary quantum mechanics. This is considered to be the simplest dual of a spacetime goverened by Einstein gravity [49].

[8] These operators are famously known as the Wilson loop operators

3.5.1 Construction and Motivation

Consider a quantum system made out of interactiong harmonic oscillators and Majorana fermions. Their lagrangian would have the rough form

$$\begin{aligned} L_B &\propto \sum_A \left[\dot{x}_A^2 + \omega^2 x_A^2 + \left(\sum_{B,C} F_{ABC} x_B x_C \right)^2 \right] \\ L_F &\propto \sum_A \left[\psi_A \dot{\psi}_A + i \sum_{B,C} \tilde{F}_{ABC} x_A \psi_B \psi_C \right] \end{aligned} \tag{3.48}$$

Where F_{ABC} and $\tilde{F}_{ABC}$ are coupling costants[9]. The total lagrangian would be the sum $L_B + L_F$. Notice the simplicity of construction, nothing but interacting bosonic and fermionic ocillators. The emergent spacetime is described at finite temperature, consisting of a black hole in a "box universe". The term "box universe" means a universe where the gravitational potential becomes large as we go away from the black hole horizon. Hence, all outgoing excitations will get back to the black hole as illustrated in figure 3.4. Our quantum system does not have a spatial extent, but the emergent gravity system lives in a higher dimensional spacetime, which has a spatial extent. This is important since this universe is governed by Einstein's equations. As we will see, we can use Einstein equations to deduce predictions about how the quantum system would behave at strong coupling. Moreover, we can compute the black hole quasinormal modes which gives information about the excitations around the black hole [13]. In the real world, such information could be extracted from the LIGO/VIRGO observations as done in [25]. Seeing these modes emerge from the quantum simulation of the system we are discussing motivates the believe that we are witnessing something which behave as a black hole in the laboratory.

Now we go into a deeper dive to shed more light into the arguments we made here.

[9] For the purpose of emphasizing simplicity, our discussion is quite general for now. Later on the system will have a specific set of couplings.

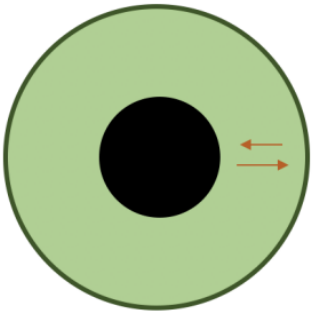

Figure 3.4: As pointed out by the red arrows, the outgoing excitation will eventually come back to the black hole due to the gravitational potential becoming larger as we move away from the horizon. this is what meant by a box universe. (Image credits: [49])

3.5.2 The Quantum Mechanics

The quantum mechanics of this model is the same as the BMN theory without gauging. To see this, we would like to give an explicit form for the bosonic and fermionic action. Starting with the bosonic action,

$$S_B = \int dt \sum_{a=1}^{N^2-1} \left[\sum_{I=1}^{9} \frac{1}{2} (\dot{X}^{aI})^2 - \frac{1}{4} \frac{\lambda}{N} \sum_{I,J=1}^{9} \Big(\sum_{b,c=1}^{N^2-1} f^a_{bc} X^{aI} X^{Jb} \Big)^2 \right] \tag{3.49}$$

where X^{aI} denotes the bosonic degrees of freedom transforming as a vector of $SO(9)$ with $I = 1, \ldots, 9$ being the $SO(9)$ vector index and $a = 1, \ldots, N^2 - 1$ is the $SU(N)$ adjoint index with structure constants f^a_{bc} coming from the $SU(N)$ generators algebra $[T_b, T_c] = iT_a f^a_{bc}$. λ is the coupling constant, and the factor of N is related to the charge of the dual black hole solution as will be seen later. We can think of the X^I as an $N \times N$ matrix with zero trace and rewrite the kinetic and interaction term of (3.49) as

$$S_B = \frac{N}{\lambda} \int dt \mathrm{Tr} \left\{ \sum_{I=1}^{9} \frac{1}{2} (\dot{X}^I)^2 + \frac{1}{4} \sum_{I,J=1}^{9} [X^I, X^J]^2 \right\} \tag{3.50}$$

note that the variables were rescaled to pull out the coupling constant.

The fermionic action has the form

$$S_F = \frac{N}{\lambda}\int dt\left[\frac{1}{2}\psi^{\alpha a}\dot{\psi}^{\alpha a} + \frac{i}{2}\psi^{\alpha a}\Gamma^I_{\alpha\beta}\psi^{\beta b}X^{Ic}f^a_{bc}\right] = \frac{N}{\lambda}\int dt\mathrm{Tr}\left[\frac{1}{2}\psi^{\alpha}\dot{\psi}^{\alpha} + \frac{1}{2}\psi^{\alpha}\Gamma^I_{\alpha\beta}[\psi^{\beta}, X^I]\right] \tag{3.51}$$

where repeated indecies are summed. The fermions, $\psi^{\alpha a}$, transform as a real 16 component spinor under $SO(9)$ and are also in the adjoint representation of $SU(N)$ with $\alpha = 1, \ldots, 16$. In the second expression, ψ^α is thought of as a matrix with $SU(N)$ indecies, $\psi^\alpha = (\psi^\alpha)^i_j$. The gamma matrices, $\Gamma^I_{\alpha\beta}$ are real and symmetric $SO(9)$ matrecies, obeying clifford algebra $\{\Gamma^I, \Gamma^J\} = 2\delta^{IJ}$.

The bosonic and fermionic degrees of freedom in (3.49) and (3.51) are related through supersymmetry, which will not be discussed in detail here. The punch line is this: the full action $S_B + S_F$ is fixed by all these symmetries up to the coupling constant λ. This constant is dimensionful and has dimensions of energy cubed. Hence, the only relevant quantity is the dimensionless ratio of λ to some other relevant energy scale. For instance, when the system is considered at finite temperature, the relevant ratio is $T/\lambda^{1/3}$. Now, we would like to add another term to the action which reinstates the harmonic oscillator frequencies

$$S_\omega = -\frac{N}{\lambda}\int dt\mathrm{Tr}\left[2\omega^2\sum_{I=1}^{3}(X^I)^2 + \frac{\omega^2}{2}\sum_{I=4}^{9}(X^I)^2 + \frac{3i}{4}\omega\psi\Gamma^1\Gamma^2\Gamma^3\psi + 2i\omega\sum_{I,J,K=1}^{3}\epsilon_{IJK}X^IX^IX^k\right] \tag{3.52}$$

which breaks the symmetry, $SO(9) \to SO(3)\times SO(6)$, indeed this is the same symmetry group of the BMN model. ϵ_{IJK} is the typical epsilon tensor in three dimensions. Having this term added, we see that the full action $S_B + S_F + S_\omega$ is simply describing a collection of interacting fermionic and bosonic oscillators. It is worth mentioning that the terms in (3.52) have helped in some other numerical computations [55].

We are interested in the regime where the effective coupling is strong (i.e. $\lambda/T^3 \gg 1$), this means

$$\omega \ll T \ll \lambda^{1/3}, \quad N^{-5/9}\lambda^{1/3} \ll T, \quad N \gg 1 \tag{3.53}$$

in which the system is strongly coupled. These conditions involve the temperature T because the dimensionless effective coupling at temperature T is given by λ/T^3. We see that the effective coupling is N independent, this is due to the N terms in (3.50) & (3.51) being chosen to cancel the factors of N that arise in the effective coupling. For high temperatures with $\lambda/T^3 \ll 1$, the system is weakly coupled and hence not interesting. The interesting features emerge as the coupling become strong. the second condition in (3.53) is concerned with the gravity dual that will be discussed shortly.

3.5.3 The Gravity dual

The gravity dual of this system is a black hole solution in a ten dimensional spacetime. The $SO(9)$ symmetry is manifested in this solution as the rotations on an 8 dimensional sphere. The black hole is a solution of an action with the Einsten term, a Maxwell term and a scalar field

$$S = \frac{1}{16\pi G_N}\int d^{10}x\sqrt{g}\left[R - \frac{1}{2}(\nabla\phi)^2 - \frac{e^{\frac{3}{2}\phi}}{4}F_{\mu\nu}F^{\mu\nu} + \dots\right] \tag{3.54}$$

The dots denote some other fields which will be zero for our solution. Note that the scalar field sets the Maxwell field coupling, $e^{\frac{3}{2}\phi}$.

The simplest solution of this action is the ten dimensional Schwarzschild solution

$$ds^2 = -f dt^2 + \frac{dr^2}{f} + r^2 d\Omega_8^2, \quad f = 1 - \frac{r_s^7}{r^7}, \quad F_{\mu\nu} = 0, \quad \phi = \text{constant} \tag{3.55}$$

Where $d\Omega_8^2$ describes the unit radius metric on the eight dimensional sphere. The solution (3.55) is similar to the Well-known four dimensional Schwarzschild solution with the two spheres replaced by an eight sphere, and $1/r \to 1/r^7$ in the metric since it is the solution to Laplace equation in nine spatial dimensions. Unfortunately, a quantum mechanical description of this simple solution is not known. Hence, a slightly more complicated solution must be considered. Namely, a charged black hole solution. The relation between its charge and the electric flux on

the sphere can be given by Gauss law

$$N = \frac{1}{16\pi G_N}\int_{S^8} e^{\frac{3}{2}\phi} * F = \frac{1}{16\pi G_N}\int_{S^8} e^{\frac{3}{2}\phi}\vec{E}\cdot d\vec{S} \tag{3.56}$$

where N is an integer because of charge quantization. This charge, N, is the same integer N of the $SU(N)$ discussed in the quantum theory. This charged black hole solution is characterized by a few parameters, the charge N, the mass and the value of ϕ at infinity [39]. Notice that ϕ is no longer constant since the flux in (3.56) depend on the coupling.

The regime we are interested in is when the mass, of this charged black hole, is near its lowest possible value for a given charge N. The final form of the metric and scalar field, which is gauged by (3.56), is

$$ds^2 = \sqrt{N}\frac{C^{1/8}}{2\pi}\rho^{9/20}\left[\frac{4}{25}\left(-\rho^2 h d\tau^2 + \frac{d\rho^2}{\rho^2 h}\right) + d\Omega_8^2\right], \quad e^{\phi} = \frac{(2\pi)^2 C^{3/4}}{N\rho^{\frac{21}{10}}} \tag{3.57}$$

where

$$h = 1-\left(\frac{\rho_0}{\rho}\right)^{\frac{14}{5}}, \quad C = 240\pi^5, \quad \tau = \frac{5}{2}\frac{\lambda^{1/3}t}{\sqrt{C}}, \quad G_N = 8\pi^6 \tag{3.58}$$

in (3.58) t should be viewed as being normalized in similar fashion to the quantum mechanical system. Also note that λ here is the same λ that was identified as the coupling constant in the quantum theory.

This metric has a number of important features:

- The over all factor of g_{tt} goes to zero at the horizon, $\rho = \rho_0$, and increases monotonically when $\rho \to \infty$. This can be viewed as a relativistic analog of a gravitational potential in which the particle can not escape due to the ever-increasing potential as the particle moves away from the horizon. It is in that sense we describe this black hole as being in a box. Where the walls of this box are determined by this increasing gravitational potential.

- The metric has a factor of $\sqrt{N}$ which gives an overall factor of N^2 when inserted to the action (3.54), keeping in mind that we are in 10 dimensions. Hence, N^2 is the relevant parameter to think about to make the gravitational dual weakly coupled. In other words,

N must be large. This is equivalent to saying that the metric (3.57) is in Planck units. Hence, as explained in previous sections[10], we need to consider large N for the curvature to be small.

- The parameter ρ_0 can be given in terms of temperature by using Hawking's formula

$$\frac{T}{\lambda^{1/3}} = \frac{7\rho_0}{a\pi\sqrt{C}} \tag{3.59}$$

where the temperature is set by the condition that the euclidean version of the metric with periodic time $t_E \sim t_e + \frac{1}{T}$ should have no singularity at the horizon. We are able to calculate the entropy in relation to the temperature, which is equal to:

$$S = \frac{Area}{4G_N} = \tilde{C}N^2\left(\frac{T}{\lambda^{(1/3)}}\right)^{9/5}, \quad \tilde{C} = 4^{13/5}15^{2/5}\left(\frac{\pi}{7}\right)^{14/5} \tag{3.60}$$

Using this result, we can deduce other thermodynamic quantities like the energy and the free energy. The entropy's dependence on temperature follows a straightforward power law pattern. Moreover, the solution (3.57) exhibits an asymptotic scaling symmetry. When $t \to \gamma t$ and $\rho \to \rho/\gamma$, the metric undergoes a rescaling by a factor of $\gamma^{-9/20}$. While the entire action experiences an overall rescaling by $\gamma^{-9/5}$, which accounts for the temperature variation in (3.60). Additionally, since the action undergoes rescaling, this implies that the equations of motion remain unchanged (i.e. invariant). Consequently, physical observables exhibit straightforward scaling properties. In simpler terms, this solution signifies a critical system manifesting scaling behavior. This isn't an exact scaling symmetry of the quantum theory, but it constitutes a scaling symmetry of the classical equations. From the standpoint of the classical theory (i.e. large N limit), this scaling symmetry is as good as a true scaling symmetry. Notably, correlation functions of specific local boundary perturbations exhibit a power law pattern over time, in the fashion $\langle O(t)O(0)\rangle \propto t^{-2\nu}$ where ν depends on the specific operator [69]. In essence, the gravity solution says that the quantum system discussed earlier develops a distinctive critical behavior at strong coupling when $\lambda/T^3 \gg 1$. It's essential to note that the action and

[10] Section (3.2.1)

the metric we discussed are well-suited for ρ values significantly smaller than one. The constraint $\rho \ll 1$, which is not immediately apparent from (3.57), originates from effects present in the comprehensive string theory description, which we've excluded here for the sake of simplicity. Thankfully, when temperatures are relatively low, $T \ll \lambda^{1/3}$, we find that $\rho_0 \ll 1$. Consequently, the horizon, along with its environment, lies within a region that we can accurately describe using gravity alone. The limitation on the upper temperature range in (3.53) follows from this condition. Remarkably, this temperature regime in which the metric can be trusted coincides precisely with the strongly coupled regime of the matrix model.

The solution presented thus far holds true under the condition that $\omega \ll T$. The gravitational solution for a more general scenario, i.e. $\omega \sim T$, can be considered [19]. Although specifics will not be provided here. This broader solution involves more fields. Additionally, phase transitions occur when $\omega \sim T$. While we've primarily focused on the regime (3.53) for conceptual clarity. However, for the purposes of simulating black holes, both quantum and classical, we can indeed consider a scenario where ω and T are comparable.

3.5.4 The possibility of a quantum simulation

In a previous study [55], the gravity-based prediction (3.60) regarding entropy was subjected to a numerical montecarlo computation within the quantum mechanical system. This was carried out for specific values of T, ω, and N. Namely:

$$\frac{T}{\lambda^{1/3}} = 0.3, \quad \frac{\omega}{T} = 0.8, \quad N = 16 \tag{3.61}$$

The outcome demonstrated a deviation of merely 13% from the gravity prediction (3.60), falling well within the numerical margin of error. For the parameters specified in (3.61), a rough estimation can be made regarding the number of qubits required for a quantum simulation of the model within a range where agreement with gravity becomes apparent. A tentative calculation involves $8N^2$ qubits attributed to the $16N^2$ Majorana fermions. As for bosons, although the

Hilbert space is of infinite dimension, the most crucial excitation levels are expected to fall within the range of $n \sim \lambda^{1/3}/\omega$. Thus, the expected number of qubits would be

$$n_q \sim N^2 \left[8 + 9 \log_2 \left(\frac{\lambda^{1/3}}{\omega} \right) \right] \sim 7000, \quad \text{for} \quad N = 16, \quad \frac{\lambda^{1/3}}{\omega} \sim 4 \tag{3.62}$$

This quantity falls within the same order of magnitude as the count of logical qubits required to perform integer factorization at a quicker pace than a classical computer [64]. Naturally, one should anticipate the presence of error correction overhead. However, our particular scenario might involve less demanding error correction requirements due to our focus on a finite-temperature setting. In essence, a quantum computer capable of breaking RSA encryption might very well possess the capability to simulate black holes! In this regard, a quantum simulation would involve testing additional observables, including predictions for quasi-normal mode frequencies and correlation functions of operators. Moreover, it could investigate inquiries far removed from equilibrium, like the emergence of a black hole or its subsequent evaporation. On a more intriguing note, such simulation could potentially offer insights into how the geometry of the emergent spacetime is intricately encoded within the quantum state of the quantum mechanical system. It is important to highlight that the "universe" being described by the quantum system is essentially quite diminutive. Its effective size, measured in Planck units, is considerably modest and doesn't approach the vast expanse of our observable universe. To illustrate the disparity, we can contrast the entropy of our universe, which is on the order of $S_{\text{our}} \propto 10^{122}$, with the entropy outlined in (3.60), which approximates $S \sim 340$ for the values provided in (3.61). Another hurdle of quantum simulation involves the count of gates or basic operations required, which can be estimated as follows. The Hamiltonian is a sum of numerous terms. The quartic term ,(3.50, involves $9^2 \times N^4$ terms, where the 9^2 arises from the summation over I and J indices, and N^4 from the $SU(N)$ indices. Similarly, the cubic term from (3.51) involves $16^2 \times 9 \times N^3$ terms. These terms collectively amount to approximately 10^7 for the specified parameters in (3.61). The inclusion of fermion operators result to an additional overhead of $\log_2(16N2)$ when expressed in qubit terms[14]. Moreover, for the creation and annihilation operators of bosons, a substantial overhead of order $\lambda^{1/3}/\omega$is anticipated. These factors add up to an approximate count of 10^8 , representing the total gates required to implement the

Hamiltonian.

To establish the thermal state, we would need to apply the Hamiltonian across a number of time steps, at least of order $\lambda^{1/3}/T$. Remarkably, this gate count seems to be comparable to the number required for breaking RSA encryption, at least considering these approximations.

Chapter 4

What is next

Since we already talked about models of holographic quantum gravity, its important to shed more light on the significant role played by quantum computers. In the last section of chapter 3 we had a taste of the importance of quantum simulation and its relation to quantum gravitational theories. In this chapter we would like to dive a little deeper, discussing the state quantum computers are in today and what to expect next.

let's first understand the concept of quantum simulation. Quantum computers leverage the principles of quantum mechanics to process information in a fundamentally different way from classical computers. At the heart of quantum computing is the qubit, the quantum analog of the classical bit. Unlike classical bits, which can only represent 0 or 1, qubits can exist in a superposition of states, enabling them to represent a vast array of information simultaneously.

Quantum simulation harnesses this unique feature to replicate and study complex quantum systems that would be impractical or impossible to simulate using classical computers. The ability to explore the quantum behaviors of particles, molecules, and even entire quantum field theories has immense implications for fields ranging from materials science to quantum chemistry.

The study of the aforementioned models in the last chapter involves grappling with plenty of quantum degrees of freedom and intricate interactions. Classical computational methods

often fall short in accurately capturing the quantum behaviors of these systems. Solving them classically may require an exponential amount of computational resources, rendering them computationally intractable.

This is where quantum computers come into play. Quantum simulation offers a promising path to explore and comprehend the quantum dynamics of holographic models efficiently. Namely, quantum computers have a certain number of promised advantages:

1. Efficient Simulation: Quantum computers can efficiently simulate complex quantum systems, including those described by holographic models, by exploiting quantum parallelism. This enables researchers to study the quantum behaviors of these models more effectively.

2. Insights into Quantum Gravity: Holographic models like BFSS and BMN hold the key to understanding fundamental aspects of quantum gravity. Quantum simulations can provide insights into the quantum gravity phenomena embedded within these models, potentially shedding light on the nature of spacetime and black holes.

3. Ungauged Models: Beyond BFSS and BMN, ungauged models with their unique complexities can also be explored using quantum simulations. These models, which may lack certain symmetries, are equally challenging to study classically.

While the potential of quantum simulation in the context of holographic models is undeniably exciting, it is essential to acknowledge the challenges that lie ahead. Building and operating practical quantum computers is still in its infantile stage, and they face hurdles related to error correction, scalability, and noise.

Nonetheless, as quantum hardware and algorithms advance, the capability of quantum computers to simulate and explore the quantum dynamics of holographic models will likely expand. This promises not only a deeper understanding of quantum gravity but also potential breakthroughs in related fields, such as condensed matter physics and quantum chemistry.

The importance of developing quantum computers can not be denied [64]. we would like to give a taste of how important the development of quantum computers is .

The cryptographic protocols we currently rely on to safeguard our online privacy could be at risk from future quantum computers. In response to this threat, researchers are actively developing "quantum-resistant" protocols. These protocols are founded on computational problems that we believe would remain challenging even for quantum computers. An alternative avenue is quantum cryptography, where quantum states are exchanged within a quantum communication network. The security of quantum communication hinges on the principle that any attempt to eavesdrop on quantum communication unavoidably disturbs the system, making any such intrusion detectable. (Quantum cryptography is a fascinating aspect of quantum technology in its own right [78, 8], but it falls outside the scope of our discussion.) The choice between these approaches may depend on the specific requirements of the user [52].

Quantum computing represents such a profound departure from conventional information processing methods that its long-term implications are difficult to predict. However, based on our current understanding of quantum computing's capabilities, using quantum computers to simulate quantum systems remains the most promising application with far-reaching potential. Enhanced techniques in computational quantum chemistry, for instance, may eventually yield substantial advancements in fields like pharmaceuticals, agriculture (e.g., nitrogen fixation), and environmental sustainability (including energy storage, production, and carbon sequestration) [51].

In contrast, while algorithms for integer factoring will likely disrupt electronic commerce in the near future, its long-term impact may not be as profound. It's crucial to highlight that quantum computers have limitations. Notably, we don't anticipate quantum computers efficiently solving exact solutions to NP-hard[1] optimization problems [7]. While there exists a general approach to expedite exhaustive search for solutions using quantum computers (known as Grover's algorithm), the acceleration in this case is quadratic [30], meaning that a quantum computer can find a solution in time proportional to the square root of the time required by a classical computer. Assuming both the classical and quantum computers operate at the same

[1] NP-hard, or non-deterministic polynomial-time hardness, is the defining property of a class of problems that are informally "at least as hard as the hardest problems in NP". For example, a problem H is NP-hard when every problem L in NP can be reduced in polynomial time to H; that is, assuming a solution for H takes 1 unit time, H's solution can be used to solve L in polynomial time [45].

clock speed (performing the same number of operations per second), a quantum computer can find a solution that is $2n$ bits long in the time it takes a classical computer to find a solution that is n bits long, for large n. This quadratic speed-up may have future importance.

However, for tasks like factoring large numbers or simulating quantum systems, the speed-up achieved by quantum computers is far more dramatic. The runtime for simulating an n-qubit quantum system using a classical computer, particularly in challenging scenarios, grows exponentially with n. In contrast, the runtime for simulating the same system on a quantum computer scales as a power of n. This discrepancy is a game-changing advantage.

4.1 Quantum computers today

It's essential to highlight that, as of now, quantum computers are not yet fully practical. Over the past four decades, various approaches to constructing quantum hardware have emerged and advanced. However, both the number of qubits (quantum bits) and the accuracy of our quantum processors remain relatively limited. A notable milestone in 2019 was achieved by the Google AI Quantum group [24], known as "quantum computational supremacy" [34, 62].

One of the profound claims about quantum physics is that classical systems generally cannot efficiently simulate quantum systems. This is a fundamental distinction between the quantum and classical realms, and validating it experimentally is of great importance. Can we identify a task performed by a quantum computer that would require an unfeasibly long time on any existing classical computer?

Using superconducting quantum technology, the Google group created a programmable quantum computer named Sycamore, featuring 53 operational qubits arranged in a two-dimensional array. They executed up to 20 layers of two-qubit gates and measured all the qubits at the end. Due to potential hardware errors, the final measurement provided the correct output only once in 500 runs. However, by repeating the computation millions of times in just a few minutes, they obtained a statistically significant result. Simulating what Sycamore achieved in a few minutes would take at least several days on the most powerful classical supercomputer

currently available [40]. Moreover, as the number of qubits increases, the cost of classical simulation grows exponentially, making it increasingly impractical. Sycamore, a single chip nestled inside a dilution refrigerator, outperforms a classical supercomputer that occupies two tennis courts and consumes megawatts of power. This illustrates quantum computing's remarkable capabilities.

Admittedly, the specific task accomplished by Sycamore may not have immediate practical applications beyond demonstrating quantum computational supremacy. However, it demonstrates that quantum hardware is sufficiently functional to produce meaningful results in scenarios where classical simulation is immensely challenging. This encourages further exploration for more meaningful applications.

The term "NISQ" (Noisy Intermediate-Scale Quantum) has emerged to describe this new quantum era [63]. "Intermediate scale" signifies that today's quantum devices with over 50 well-controlled qubits cannot be efficiently simulated by the most powerful existing classical supercomputers. "Noisy" reminds us that these devices are not error-corrected and are limited by noise, which affects their computational power. For physicists, NISQ technology is exciting because it provides new tools to explore highly complex many-particle quantum systems in a previously inaccessible regime. It may also have applications beyond physics, but that remains uncertain. NISQ is not expected to revolutionize the world on its own, at least not immediately. Instead, it represents a step toward the development of more powerful quantum technologies in the future.

In the most advanced multi-qubit quantum processors currently available, the probability of a two-qubit quantum gate making a significant error is slightly less than 1%. This limitation led to the inability of the 53-qubit Sycamore device to execute circuits with more than 20 time steps. We currently lack compelling arguments that a quantum computation with around 100 qubits and fewer than 100 time steps can effectively solve practical problems.

One approach to leverage NISQ devices is to seek approximate solutions to optimization problems using a hybrid quantum/classical approach. This strategy relies heavily on powerful classical processors and attempts to enhance their capabilities with a NISQ co-processor. However,

it remains uncertain whether this hybrid method can outperform the best classical hardware running the most efficient classical algorithms for solving similar problems. This is a substantial challenge, considering that classical methods have undergone decades of refinement, while NISQ processors are just becoming available now. Nevertheless, we must explore and experiment to determine its effectiveness. Vibrant discussions are ongoing among potential users, hardware providers, and quantum algorithm experts. As we gain experience with NISQ technology, we will gain insights into its performance and potential applications.

Despite their notable limitations, NISQ processors have the potential to prepare and investigate exotic quantum states that were previously beyond the reach of laboratory experiments.

Classical computers face significant challenges when simulating quantum dynamics, particularly in predicting the evolution of highly entangled quantum states over time. Quantum computers possess a distinct advantage in this regard. It's worth recalling that the field of classical chaos theory, which deals with the extreme sensitivity of classical dynamical systems to initial conditions (e.g., weather prediction challenges), made significant progress in the 1960s and 1970s once classical computers enabled the simulation of chaotic systems. Similarly, the emerging ability to simulate chaotic quantum systems, characterized by the rapid spread of entanglement, is expected to advance our understanding of quantum chaos. Valuable insights may be collected even using noisy quantum devices equipped with approximately 100 qubits.

It's important to distinguish between analog and digital quantum simulation. Analog quantum simulation involves systems with numerous qubits whose dynamics mimic those of the model system under investigation. Conversely, digital quantum simulation entails gate-based universal quantum computers that can simulate any desired physical system when appropriately programmed and can serve various purposes.

Analog quantum simulation has been a vibrant field of research for the past two decades [42, 29]. Digital quantum simulation with general-purpose circuit-based quantum computers is still in its early stages. Some experimental platforms can serve both analog and digital simulation purposes, while others, like trapped neutral atoms and molecules, excel as analog simulators. Analog quantum simulators have grown increasingly sophisticated and are already employed to

study quantum dynamics in regimes that may challenge classical simulators [12, 79]. They can also create highly entangled equilibrium states of quantum matter and investigate their static properties [18, 53, 70].

However, analog quantum simulators face limitations due to imperfect control, as the actual quantum system approximates the target system of interest. As a result, analog simulators are best suited for studying universal features—properties relatively robust against minor sources of error. A significant research challenge is identifying accessible quantum system properties that withstand errors while remaining challenging for classical simulations.

It's foreseeable that analog quantum simulators will eventually be surpassed by digital quantum simulators, which can be rigorously controlled using quantum error correction. Nevertheless, analog quantum simulators will likely remain relevant for many years due to their lower overhead cost. Therefore, in the quest for near-term quantum technology applications, the potential of analog quantum simulators should not be underestimated.

In the near term, circuit-based simulations of quantum matter may be cost-prohibitive, especially for realistic simulations of many-particle systems requiring numerous gates. However, circuit-based methods offer greater flexibility in studying various Hamiltonians and preparing initial states. Therefore, it's crucial to explore both digital and analog simulation approaches, recognizing that experience with near-term digital simulators will establish foundations for more ambitious simulations in the future. This same perspective applies to broader applications of NISQ technology.

4.2 Quantum computers tomorrow

In the NISQ era, quantum devices will not benefit from the protective shield of quantum error correction, and the presence of noise significantly constrains the scale of computations that can be reliably performed using NISQ technology. Looking to the future, we anticipate overcoming these noise-related limitations through the implementation of quantum error correction (QEC) and the development of fault-tolerant quantum computing (FTQC). However, it's essential

to acknowledge that QEC comes with a substantial overhead in terms of both the number of qubits and logic gates required [27, 16]. This overhead depends on the specific algorithms being executed and the quality of the hardware.

To illustrate, if we assume an error rate of approximately 0.1% per entangling two-qubit gate (which represents an improvement over current hardware), running high-impact applications in quantum chemistry or materials science could necessitate more than one hundred thousand physical qubits [44, 15]. Even though the quantum system explored previously needs the scale of a thousands of qubits as seen in (3.62), this projection signifies a considerable leap from where we foresee quantum technology in the next few years, with a few hundred physical qubits at our disposal. Achieving the scale of hundreds of thousands or even millions of physical qubits will likely be a gradual process and may take a significant amount of time.

While quantum computing may hold significant importance to the advancement of the holographic models discussed in chapter 3, this impact might still be several decades away. The exact timeline remains uncertain, considering that quantum technology is still in its early stages, with various competing approaches. It's important to acknowledge that an unforeseen breakthrough could potentially reshape the landscape and accelerate progress in unexpected ways.

Bibliography

[1] Ofer Aharony, Oren Bergman, Daniel Louis Jafferis, and Juan Maldacena. N = 6 superconformal chern-simons-matter theories, m2-branes and their gravity duals. *Journal of High Energy Physics*, 2008(10):091–091, oct 2008.

[2] Yuhma Asano, Veselin G. Filev, Samuel Kováčik, and Denjoe O'Connor. The non-perturbative phase diagram of the BMN matrix model. *Journal of High Energy Physics*, 2018(7), jul 2018.

[3] T. Banks, W. Fischler, S. H. Shenker, and L. Susskind. M theory as a matrix model: A conjecture. *Physical Review D*, 55(8):5112–5128, apr 1997.

[4] James M. Bardeen, B. Carter, and S. W. Hawking. The Four laws of black hole mechanics. *Commun. Math. Phys.*, 31:161–170, 1973.

[5] Jacob D. Bekenstein. Black holes and entropy. *Phys. Rev. D*, 7:2333–2346, 1973.

[6] Jacob D. Bekenstein. Generalized second law of thermodynamics in black hole physics. *Phys. Rev. D*, 9:3292–3300, 1974.

[7] Charles H. Bennett, Ethan Bernstein, Gilles Brassard, and Umesh Vazirani. Strengths and weaknesses of quantum computing. *SIAM Journal on Computing*, 26(5):1510–1523, oct 1997.

[8] Charles H. Bennett and Gilles Brassard. Quantum cryptography: Public key distribution and coin tossing. *Theoretical Computer Science*, 560:7–11, dec 2014.

[9] David Berenstein, Juan Maldacena, and Horatiu Nastase. Strings in flat space and pp waves from script n = 4 super yang mills. *Journal of High Energy Physics*, 2002(04):013–013, apr 2002.

[10] Evan Berkowitz, Enrico Rinaldi, Masanori Hanada, Goro Ishiki, Shinji Shimasaki, and Pavlos Vranas and. Precision lattice test of the gauge/gravity duality at large N. *Physical Review D*, 94(9), nov 2016.

[11] Evan Berkowitz, Enrico Rinaldi, Masanori Hanada, Goro Ishiki, Shinji Shimasaki, and Pavlos Vranas. Supergravity from d0-brane quantum mechanics, 2016.

[12] Hannes Bernien, Sylvain Schwartz, Alexander Keesling, Harry Levine, Ahmed Omran, Hannes Pichler, Soonwon Choi, Alexander S. Zibrov, Manuel Endres, Markus Greiner, Vladan Vuletić, and Mikhail D. Lukin. Probing many-body dynamics on a 51-atom quantum simulator. *Nature*, 551(7682):579–584, nov 2017.

[13] Anna Biggs and Juan Maldacena. Scaling similarities and quasinormal modes of d0 black hole solutions, 2023.

[14] Sergey B. Bravyi and Alexei Yu. Kitaev. Fermionic quantum computation. *Annals of Physics*, 298(1):210–226, may 2002.

[15] Earl T Campbell. Early fault-tolerant simulations of the hubbard model. *Quantum Science and Technology*, 7(1):015007, nov 2021.

[16] Earl T. Campbell, Barbara M. Terhal, and Christophe Vuillot. Roads towards fault-tolerant universal quantum computation. *Nature*, 549(7671):172–179, sep 2017.

[17] Simon Catterall and Greg van Anders. First results from lattice simulation of the PWMM. *Journal of High Energy Physics*, 2010(9), sep 2010.

[18] Christie S. Chiu, Geoffrey Ji, Annabelle Bohrdt, Muqing Xu, Michael Knap, Eugene Demler, Fabian Grusdt, Markus Greiner, and Daniel Greif. String patterns in the doped hubbard model. *Science*, 365(6450):251–256, jul 2019.

[19] Miguel S. Costa, Lauren Greenspan, João Penedones, and Jorge E. Santos. Thermodynamics of the BMN matrix model at strong coupling. *Journal of High Energy Physics*, 2015(3), mar 2015.

[20] ULF H. DANIELSSON, GABRIELE FERRETTI, and BO SUNDBORG. D-PARTICLE DYNAMICS AND BOUND STATES. *International Journal of Modern Physics A*, 11(31):5463–5477, dec 1996.

[21] Nadav Drukker, Marcos Mariño, and Pavel Putrov. From weak to strong coupling in ABJM theory. *Communications in Mathematical Physics*, 306(2):511–563, may 2011.

[22] Veselin G. Filev and Denjoe O'Connor. The BFSS model on the lattice. *Journal of High Energy Physics*, 2016(5), may 2016.

[23] A. Fotopoulos and T. R. Taylor. Remarks on two-loop free energy in N=4 supersymmetric yang-mills theory at finite temperature. *Physical Review D*, 59(6), feb 1999.

[24] Ryan Babbush Dave Bacon Joseph C Bardin Rami Barends Rupak Biswas Sergio Boixo Fernando GSL Brandao David A Buell et al. Frank Arute, Kunal Arya. Quantum supremacy using a programmable superconducting processor. *Nature*, 574:505–510, 2019.

[25] Abhirup Ghosh, Richard Brito, and Alessandra Buonanno. Constraints on quasinormal-mode frequencies with LIGO-virgo binary–black-hole observations. *Physical Review D*, 103(12), jun 2021.

[26] Steven B. Giddings. Why aren't black holes infinitely produced? *Physical Review D*, 51(12):6860–6869, jun 1995.

[27] Daniel Gottesman. An introduction to quantum error correction and fault-tolerant quantum computation, 2009.

[28] Michael B. Green, John H. Schwarz, and Lars Brink. N=4 Yang-Mills and N=8 Supergravity as Limits of String Theories. *Nucl. Phys. B*, 198:474–492, 1982.

[29] M. Greiner, O. Mandel, T. Rom, A. Altmeyer, A. Widera, T.W. Hänsch, and I. Bloch. Quantum phase transition from a superfluid to a mott insulator in an ultracold gas of

atoms. *Physica B: Condensed Matter*, 329-333:11–12, 2003. Proceedings of the 23rd International Conference on Low Temperature Physics.

[30] Lov K. Grover. Quantum mechanics helps in searching for a needle in a haystack. *Physical Review Letters*, 79(2):325–328, jul 1997.

[31] S. S. Gubser, I. R. Klebanov, and A. W. Peet. Entropy and temperature of black 3-branes. *Physical Review D*, 54(6):3915–3919, sep 1996.

[32] Steven S. Gubser, Igor R. Klebanov, and Arkady A. Tseytlin. Coupling constant dependence in the thermodynamics of n = 4 supersymmetric yang-mills theory. *Nuclear Physics B*, 534(1-2):202–222, nov 1998.

[33] D. Harlow. Jerusalem lectures on black holes and quantum information. *Reviews of Modern Physics*, 88(1), feb 2016.

[34] Aram W. Harrow and Ashley Montanaro. Quantum computational supremacy. *Nature*, 549(7671):203–209, sep 2017.

[35] S. W. Hawking. Gravitational radiation from colliding black holes. *Phys. Rev. Lett.*, 26:1344–1346, 1971.

[36] S. W. Hawking. Particle Creation by Black Holes. *Commun. Math. Phys.*, 43:199–220, 1975. [Erratum: Commun.Math.Phys. 46, 206 (1976)].

[37] Gary T. Horowitz and Emil J. Martinec. Comments on black holes in matrix theory. *Physical Review D*, 57(8):4935–4941, apr 1998.

[38] Gary T. Horowitz and Joseph Polchinski. Correspondence principle for black holes and strings. *Physical Review D*, 55(10):6189–6197, may 1997.

[39] Gary T. Horowitz and Andrew Strominger. Black strings and P-branes. *Nucl. Phys. B*, 360:197–209, 1991.

[40] Cupjin Huang, Fang Zhang, Michael Newman, Junjie Cai, Xun Gao, Zhengxiong Tian, Junyin Wu, Haihong Xu, Huanjun Yu, Bo Yuan, Mario Szegedy, Yaoyun Shi, and Jianxin Chen. Classical simulation of quantum supremacy circuits, 2020.

[41] Nissan Itzhaki, Juan M. Maldacena, Jacob Sonnenschein, and Shimon Yankielowicz. Supergravity and the large N limit of theories with sixteen supercharges. *Physical Review D*, 58(4), jul 1998.

[42] D. Jaksch, C. Bruder, J. I. Cirac, C. W. Gardiner, and P. Zoller. Cold bosonic atoms in optical lattices. *Physical Review Letters*, 81(15):3108–3111, oct 1998.

[43] Daisuke Kadoh and Syo Kamata. Gauge/gravity duality and lattice simulations of one dimensional sym with sixteen supercharges, 2015.

[44] Ian D. Kivlichan, Craig Gidney, Dominic W. Berry, Nathan Wiebe, Jarrod McClean, Wei Sun, Zhang Jiang, Nicholas Rubin, Austin Fowler, Alá n Aspuru-Guzik, Hartmut Neven, and Ryan Babbush. Improved fault-tolerant quantum simulation of condensed-phase correlated electrons via trotterization. *Quantum*, 4:296, jul 2020.

[45] D. E. Knuth. Postscript about np-hard problems. *SIGACT News*, 6(2):15–16, apr 1974.

[46] Juan Maldacena. Wilson loops in large N field theories. *Physical Review Letters*, 80(22):4859–4862, jun 1998.

[47] Juan Maldacena. *International Journal of Theoretical Physics*, 38(4):1113–1133, 1999.

[48] Juan Maldacena. The gauge/gravity duality, 2014.

[49] Juan Maldacena. A simple quantum system that describes a black hole. 3 2023.

[50] Juan Maldacena and Alexey Milekhin. To gauge or not to gauge? *Journal of High Energy Physics*, 2018(4), apr 2018.

[51] Sam McArdle, Suguru Endo, Alá n Aspuru-Guzik, Simon C. Benjamin, and Xiao Yuan. Quantum computational chemistry. *Reviews of Modern Physics*, 92(1), mar 2020.

[52] Michele Mosca. Cybersecurity in an era with quantum computers: Will we be ready? *IEEE Security Privacy*, 16(5):38–41, 2018.

[53] Biswaroop Mukherjee, Parth B. Patel, Zhenjie Yan, Richard J. Fletcher, Julian Struck, and Martin W. Zwierlein. Spectral response and contact of the unitary fermi gas. *Physical Review Letters*, 122(20), may 2019.

[54] Robert C Myers. Dielectric-branes. *Journal of High Energy Physics*, 1999(12):022–022, dec 1999.

[55] Stratos Pateloudis, Georg Bergner, Masanori Hanada, Enrico Rinaldi, Andreas Schäfer, Pavlos Vranas, Hiromasa Watanabe, and Norbert Bodendorfer. Precision test of gauge/gravity duality in d0-brane matrix model at low temperature. *Journal of High Energy Physics*, 2023(3), mar 2023.

[56] Jorge Pinochet. The hawking temperature, the uncertainty principle and quantum black holes. *Physics Education*, 53(6):065004, aug 2018.

[57] J. Polchinski. *String theory. Vol. 1: An introduction to the bosonic string*. Cambridge Monographs on Mathematical Physics. Cambridge University Press, 12 2007.

[58] J. Polchinski. *String theory. Vol. 2: Superstring theory and beyond*. Cambridge Monographs on Mathematical Physics. Cambridge University Press, 12 2007.

[59] Joseph Polchinski. Dirichlet branes and ramond-ramond charges. *Physical Review Letters*, 75(26):4724–4727, dec 1995.

[60] Joseph Polchinski, Shyamoli Chaudhuri, and Clifford V. Johnson. Notes on d-branes, 1996.

[61] John Preskill. Do black holes destroy information?, 1992.

[62] John Preskill. Quantum computing and the entanglement frontier, 2012.

[63] John Preskill. Quantum computing in the NISQ era and beyond. *Quantum*, 2:79, aug 2018.

[64] John Preskill. Quantum computing 40 years later, 2023.

[65] S.-J. Rey and J.-T. Yee. Macroscopic strings as heavy quarks: Large-n gauge theory and anti-de sitter supergravity. *The European Physical Journal C*, 22(2):379–394, nov 2001.

[66] David Schaich, Raghav G. Jha, and Anosh Joseph. Thermal phase structure of a supersymmetric matrix model. In *Proceedings of 37th International Symposium on Lattice Field Theory — PoS(LATTICE2019)*. Sissa Medialab, mar 2020.

[67] John H. Schwarz. Covariant Field Equations of Chiral N=2 D=10 Supergravity. *Nucl. Phys. B*, 226:269, 1983.

[68] Nathan Seiberg. Why is the matrix model correct? *Physical Review Letters*, 79(19):3577–3580, nov 1997.

[69] Yasuhiro Sekino and Tamiaki Yoneya. Generalized AdS–CFT correspondence for matrix theory in the large-n limit. *Nuclear Physics B*, 570(1-2):174–206, mar 2000.

[70] G. Semeghini, H. Levine, A. Keesling, S. Ebadi, T. T. Wang, D. Bluvstein, R. Verresen, H. Pichler, M. Kalinowski, R. Samajdar, A. Omran, S. Sachdev, A. Vishwanath, M. Greiner, V. Vuletić , and M. D. Lukin. Probing topological spin liquids on a programmable quantum simulator. *Science*, 374(6572):1242–1247, dec 2021.

[71] Ashoke Sen. D0 branes on t^n*andmatrixtheory*, 1997.

[72] Andrew Strominger and Cumrun Vafa. Microscopic origin of the bekenstein-hawking entropy. *Physics Letters B*, 379(1-4):99–104, jun 1996.

[73] Leonard Susskind. Some speculations about black hole entropy in string theory. pages 118–131, 10 1993.

[74] Leonard Susskind. Trouble for remnants, 1995.

[75] Leonard Susskind. The world as a hologram. *Journal of Mathematical Physics*, 36(11):6377–6396, nov 1995.

[76] Leonard Susskind. Another conjecture about M(atrix) theory, 1997.

[77] Gerard 't Hooft. A Planar Diagram Theory for Strong Interactions. *Nucl. Phys. B*, 72:461, 1974.

[78] Stephen Wiesner. Conjugate coding. *SIGACT News*, 15(1):78–88, jan 1983.

[79] J. Zhang, G. Pagano, P. W. Hess, A. Kyprianidis, P. Becker, H. Kaplan, A. V. Gorshkov, Z.-X. Gong, and C. Monroe. Observation of a many-body dynamical phase transition with a 53-qubit quantum simulator. *Nature*, 551(7682):601–604, nov 2017.